Brown GL, Curtsinger L, Brightwell JR, *et al*: Enhancement of epidermal regeneration by biosynthetic epidermal growth factor. J Exp Med 163:1319–1324, 1986

Clark RAF, Henson PM: The Molecular and Cellular Biology of Wound Repair. New York: Plenum Press, 1988; p 3–33

Dunnett CW: New tables for multiple comparisons with a control. Biometrics 20:482–491, 1964

Gailit J, Welch MP, Clark RA: TGF-beta 1 stimulates expression of keratinocyte integrins during re-epithelialization of cutaneous wounds. J Invest Dermatol 103:221–227, 1994

Gibson UEM, Heid CA, Williams A: Novel method for real time quantitative RT-PCR. Genome Res 6:995–1001, 1996

Goliger JA, Paul DL: Wounding alters epidermal connexin expression and gap junction-mediated intercellular communication. Mol Biol Cell 6:1491–1501, 1995

Hata K, Kagami H, Ueda M, Trii S, Matsuyama M: The characteristics of cultured mucosal cell sheet as a material for grafting: Comparison with cultured epidermal cell sheet. Ann Plast Surg 34:530–538, 1995

Heid CA, Stevens J, Williams PM: Real time quantitative PCR. Genome Res 6:986–994, 1996

Heldin P, Laurent TC, Heldin CH: Effect of growth factors on hyaluronan synthesis in cultured human fibroblasts. Biochem J 258:919–922, 1989

Hubner G, Brauchle M, Smola H, *et al*: Differential regulation of pro-inflammatory cytokines during wound healing in normal and glucocorticoid-treated mice. Cytokine 8:548–556, 1996

Itano N, Kimata K: Expression cloning and molecular characterization of HAS protein, a eukaryotic hyaluranan synthase. J Biol Chem 271:9875–9878, 1996a

Itano N, Kimata K: Molecular cloning of human hyaluronan synthase. Biochem Biophys Res Commun 222:816–820, 1996b

Itano N, Sawai T, Yamada Y, *et al*: Three isoforms of mammalian hyaluronan synthase have distinct enzymatic properties. J Biol Chem 274:25085–25092, 1999

Jacobson A, Brinck J, Briskin MJ, Spicer AP, Heldin P: Expression of human hyaluronan synthases in response to external stimuli. Biochem J 348:29–35, 2000

Kaback LA, Smith TJ: Expression of hyaluranan synthase messenger ribonucleic acids and their induction by interleukin-1 beta in human orbital fibroblasts: Potential insight into the molecular pathogenesis of thyroid-associated ophthalmopathy. J Clin Endocrinol Metab 84:4079–4084, 1999

Knudson W, Biswas C, Li X-Q, Nemec RE, Toole BP: The biology of hyaluronan. In: Evered D, Whelan J (eds). Ciba Foundation Symposium, Vol. 143. Chichester, UK: Wiley, 1989; p 150–169

Krejci NC, Cuono CB, Langdon RC: *In vitro* reconstitution of skin: Fibroblasts facilitate keratinocyte growth and differentiation on acellular reticular dermis. J Invest Dermatol 97:843–848, 1991

Langer R, Vacanti JP: Tissue engineering. Science 260:920–926, 1993

Leibovich SJ, Ross R: The role of the macrophage in wound repair. A study with hydrocortisone and antimacrophage serum. Am J Pathol 78:71–100, 1975

Martin P: Wound healing—Aiming for perfect skin regeneration. Science 276:75–81, 1997

Pienimaki JP, Rilla K, Fulop C, *et al*: Epidermal growth factor activates hyaluronan synthesis 2 in epidermal keratinocytes and increases pericellular and intracellular hyaluronan. J Biol Chem 276:20428–20435, 2001

Rosa F, Sargent TD, Rebbert ML, *et al*: Accumulation and decay of DG42 gene products follow a gradient pattern during Xenopus embryogenesis. Dev Biol 129:114–123, 1988

Sayo T, Sugiyama Y, Takahashi Y, *et al*: Hyaluronan synthase 3 regulates hyaluronan synthesis in cultured human keratinocytes. J Invest Dermatol 118:43–48, 2002

Shyjan A, Heldin P, Butcher E, Yoshino T, Briskin M: Functional cloning of the cDNA for a human hyaluronan synthase. J Biol Chem 271:23395–23399, 1996

Spicer AP, Augustine ML, Mcdonald JA: Molecular cloning and characterization of putative mouse hyaluronan synthase. J Biol Chem 271:23400–23406, 1996

Spicer AP, Olson JS, McDonald JA: Molecular cloning and characterization of a cDNA encoding the third putative mammalian hyaluronan synthase. J Biol Chem 272:8957–8961, 1997

Spicer AP, Mcdonald JA: Characterization and molecular evolution of a vertebrate hyaluronan synthase gene family. J Biol Chem 273:1923–1932, 1998

Sugiyama Y, Shimada A, Sayo T, Sakai S, Inoue SJ: Putative hyaluronan synthase mRNA are expressed in mouse skin and TGF-beta upregulates their expression in cultured human skin cells. J Invest Dermatol 110:116–121, 1998

Tammi R, Ripellino JA, Margolis RU, Maibach HI, Tammi M: Hyaluronate accumulation in human epidermis treated with retinoic acid in skin. J Invest Dermatol 92:326–332, 1989

Tammi R, Ripellino JA, Margolis RU, Tammi M: Localization of epidermal hyaluronic acid using the hyaluronate binding region of cartilage proteoglycan as a specific probe. J Invest Dermatol 90:412–414, 1988

Tammi R, Tammi M: Glycoforum. Online (http://www.glycoforum.gr.jp/) 1–12, 1998

Tsai CY, Hata K, Trii S, Matsuyama M, Ueda M: Contraction potency of hypertrophic scar-derived fibroblasts in a connective tissue model: *In vivo* analysis of wound contraction. Ann Plast Surg 35:638–646, 1995

Turley EA: The biology of hyaluronan. In: Evered D, Whelan J (eds). Ciba Foundation Symposium, Vol. 143. Chichester, UK: Wiley, 1989; p 121–137

Ueda M, Hata K, Horie K, Torii S: The potential of oral mucosal cells for cultured epithelium: A preliminary report. Ann Plast Surg 35:498–504, 1995

Watanabe K, Yamaguchi Y: Molecular identification of a putative human hyaluronan synthase. J Biol Chem 271:22945–22948, 1996

Weigel PH, Hascall VC, Tammi M: Hyaluronan synthases. J Biol Chem 272:13997–14000, 1997

Yamada Y, Itano N, Zako M, *et al*: The gene structure and promoter sequence of mouse hyaluronan synthase 1 (mHAS1). Biochem J 330:1223–1227, 1998

Yung S, Coles GA, Davies M: IL-1 beta, major stimulator of hyaluronan synthesis *in vitro* of human peritoneal cells: Relevance to peritonitis in CAPD. Kidney Int 50:1337–1343, 1996

Zhang W, Watson CE, Liu C, Williams KJ, Werth VP: Glucocorticoids induce a near-total suppression of hyaluronan synthase mRNA in dermal fibroblasts and in osteoblasts: A molecular mechanism contributing to organ atrophy. Biochem J 349:91–97, 2000

THE JOURNAL OF BIOLOGICAL CHEMISTRY
Vol. 279, No. 13, Issue of March 26, pp. 12346–12354, 2004
Printed in U.S.A.

Characterization of Growth Factor-binding Structures in Heparin/ Heparan Sulfate Using an Octasaccharide Library*

Received for publication, December 10, 2003
Published, JBC Papers in Press, January 5, 2004, DOI 10.1074/jbc.M313523200

Satoko Ashikari-Hada‡§, Hiroko Habuchi‡, Yutaka Kariya§, Nobuyuki Itoh¶, A. Hari Reddi‖, and Koji Kimata‡**

From the ‡Institute for Molecular Science of Medicine, Aichi Medical University, Nagakute, Aichi 480-1195, §Central Research Laboratories, Seikagaku Corp., Tateno, Higashiyamato-shi, Tokyo 207-0021, ¶Department of Genetic Biochemistry, Kyoto University Graduate School of Pharmaceutical Sciences, Yoshida-Shimoadachi, Sakyo, Kyoto 606-8501, Japan, and ‖Center for Tissue Regeneration and Repair, University of California School of Medicine, Davis, California 95817

Heparan sulfate (HS) chains interact with various growth and differentiation factors and morphogens, and the most interactions occur on the specific regions of the chains with certain monosaccharide sequences and sulfation patterns. Here we generated a library of octasaccharides by semienzymatic methods by using recombinant HS 2-*O*-sulfotransferase and HS 6-*O*-sulfotransferase, and we have made a systematic investigation of the specific binding structures for various heparin-binding growth factors. An octasaccharide (Octa-I, ΔHexA-GlcNSO$_3$-(HexA-GlcNSO$_3$)$_3$) was prepared by partial heparitinase digestion from completely desulfated *N*-resulfated heparin. 2-*O*- and 6-*O*-sulfated Octa-I were prepared by enzymatically transferring one to three 2-*O*-sulfate groups and one to three 6-*O*-sulfate groups per molecule, respectively, to Octa-I. Another octasaccharide containing 3 units of HexA(2SO$_4$)-GlcNSO$_3$(6SO$_4$) was prepared also from heparin. This octasaccharide library was subjected to affinity chromatography for interactions with fibroblast growth factor (FGF)-2, -4, -7, -8, -10, and -18, hepatocyte growth factor, bone morphogenetic protein 6, and vascular endothelial growth factor, respectively. Based upon differences in the affinity to those octasaccharides, the growth factors could be classified roughly into five groups: group 1 needed 2-*O*-sulfate but not 6-*O*-sulfate (FGF-2); group 2 needed 6-*O*-sulfate but not 2-*O*-sulfate (FGF-10); group 3 had the affinity to both 2-*O*-sulfate and 6-*O*-sulfate but preferred 2-*O*-sulfate (FGF-18, hepatocyte growth factor); group 4 required both 2-*O*-sulfate and 6-*O*-sulfate (FGF-4, FGF-7); and group 5 hardly bound to any octasaccharides (FGF-8, bone morphogenetic protein 6, and vascular endothelial growth factor). The approach using the oligosaccharide library may be useful to define specific structures required for binding to various heparin-binding proteins. Octasaccharides with the high affinity to FGF-2 and FGF-10 had the activity to release them, respectively, from their complexes with HS. Thus, the library may provide new reagents to specifically regulate bindings of the growth factors to HS.

Heparan sulfate (HS)[1] exists ubiquitously as a component of proteoglycans on cell surfaces and in extracellular matrix and basement membranes and has divergent structures and functions (1–3). HS chains are known to interact with a variety of proteins such as heparin-binding growth and differentiation factors (HBGFs), morphogens, extracellular matrix components, protease inhibitors, protease, lipoprotein lipase, and various pathogens (4–8). These interactions have been shown to play a pivotal role in various patho-physiological phenomena as well as in tissue morphogenesis, as uncovered by recent genetic studies (9–12). In some of these phenomena, the interactions of HS with certain proteins have been shown in regions of the HS with specific monosaccharide sequences and sulfation patterns. Such functional domains are thought to be generated after the sequential modification steps during the biosynthesis of HS. In these modification steps, HS *N*-deacetylase/*N*-sulfotransferases (13–16), C5 epimerase (17), HS 2-*O*-sulfotransferase (HS2ST) (18), HS 6-*O*-sulfotransferases (HS6ST) (19, 20), and HS 3-*O*-sulfotransferase (21, 22) are involved. The expression patterns of the individual modification enzymes have been shown to differ from tissue to tissue, and as a result different functional structures of HS may be generated in the different tissues. Such structural diversity introduced to HS may result in the different response of each tissue to various heparin-binding proteins.

So far, the sequences in HS that interact with FGF-1 or FGF-2 have been studied by biochemical and x-ray crystallographic analysis. It became apparent that the FGF-1-binding region was distinct from the minimal FGF-2-binding region (23–27). In addition to the studies on FGF-1 and FGF-2, the HS sequences that mediate binding and/or activation of some HBGFs have been reported in the systems including FGF-4 (23, 24), FGF-8b (28), hepatocyte growth factor (HGF) (29–31), and platelet-derived growth factor (32). These studies on the binding structures in HS appear to support the idea that each heparin-binding growth factor may recognize the respective

* This work was supported in part by Grant-in-aid for Scientific Research on Priority Areas from the Ministry of Education, Culture, Sports, Science and Technology of Japan 14082206, by a preparatory grant for research at the Matrix Glycoconjugate Group, Research Center for Infectious Disease, Aichi Medical University, and by a special research fund from Seikagaku Corp. The costs of publication of this article were defrayed in part by the payment of page charges. This article must therefore be hereby marked "*advertisement*" in accordance with 18 U.S.C. Section 1734 solely to indicate this fact.

** To whom correspondence should be addressed. Tel.: 81-52-264-4811 (ext. 2088); Fax: 81-561-63-3532; E-mail: kimata@aichi-med-u.ac.jp.

[1] The abbreviations used are: HS, heparan sulfate; FGF, fibroblast growth factor; HGF, hepatocyte growth factor; VEGF, vascular endothelial growth factor; BMP, bone morphogenetic protein; GF, growth factor; HBGF, heparin-binding growth and differentiation factor; CDSNS, completely desulfated, *N*-sulfated; 2ODS, 2-*O*-desulfated; 6ODS, 6-*O*-desulfated; GAG, glycosaminoglycan, IdoUA, L-iduronic acid; HexA, hexuronic acid; GlcNSO$_3$, *N*-sulfoglucosamine; HS2ST, heparan sulfate 2-*O*-sulfotransferase; HS6ST, heparan sulfate 6-*O*-sulfotransferase; PBS, phosphate-buffered saline; BSA, bovine serum albumin; PAPS, adenosine 3′-phosphate,5′-phosphosulfate; ELISA, enzyme-linked immunosorbent assay; HPLC, high performance liquid chromatography; h, human; Octa, octasaccharide; SPR, surface plasmon resonance.

unique structure. However, our knowledge about the heparin/HS structures involved in the interaction with a variety of HBGFs is still limited, and the greater part of the interactions between HS and the heparin-binding proteins remains to be studied. Furthermore, structural analyses of HS with binding activity for HBGFs often give different results when HS is isolated from different sources (29, 30).

In the present study, we prepared an octasaccharide library consisting of well defined sulfated octasaccharides. The library comprised 2-*O*-sulfated or 6-*O*-sulfated octasaccharides generated from CDSNS-heparin-derived octasaccharide (Octa-I) by *in vitro* reactions with HS2ST or HS6ST. By using this library, we examined the structures that were specifically bound to the various HBGFs including FGF-2, FGF-4, FGF-7, FGF-8, FGF-10, FGF-18, HGF, BMP-6, and VEGF. Our results show that these HBGFs could be classified roughly into five groups on the basis of the difference in affinity with the oligosaccharides, and offer further evidence for specific interactions between heparin-binding growth factors and the corresponding domain structures in HS. Furthermore, for a physiological relevance of this study, we demonstrated specific release of FGF-10 and FGF-2 from HS by the addition of 6-*O*-sulfated Octa-I and 2-*O*-sulfated Octa-I, respectively.

EXPERIMENTAL PROCEDURES

Materials—Completely desulfated, *N*-sulfated heparin (CDSNS-heparin), chondroitin 4-sulfate from whale cartilage, heparitinase I (*Flavobacterium heparinum*, EC 4.2.2.8), heparitinase II (*F. heparinum*, no number assigned), heparinase (*F. heparinum*, EC 4.2.2.7), 2-*O*-desulfated heparin (2ODS-heparin), 6-*O*-desulfated heparin (6ODS-heparin), and an unsaturated glycosaminoglycan disaccharide kit were obtained from Seikagaku Corp. (Tokyo, Japan). Heparin and unlabeled PAPS were purchased from Sigma. [^{35}S]PAPS was purchased from PerkinElmer Life Sciences. [^{3}H]$NaBH_4$ (36 Ci/mmol) was purchased from Amersham Biosciences. Hiload Superdex 30 HR 16/60, fast desalting column HR 10/10, Mono Q HR 5/5 and PD-10 were from Amersham Biosciences. Senshu Pak Docosil was obtained from Senshu Scientific (Tokyo, Japan). Recombinant human FGF-7, FGF-10, and FGF-18 were provided by Amgen Inc. (Thousand Oaks, CA). Recombinant human FGF-2 was purchased from Progen Biotechnic GmbH (Heidelberg, Germany). Recombinant human FGF-8 was purchased from PeproTech (Rocky Hill, NJ). Recombinant human FGF-4 was purchased from R & D Systems (Minneapolis, MN). Recombinant human HGF was purchased from Genzyme-Techne (Minneapolis, MN). Recombinant bone morphogenetic protein 6 (BMP-6) was a gift from Creative Biomolecules Inc., Hopkinton, MA, courtesy of Dr. T. K. Sampath. Recombinant human $VEGF_{165}$ was purchased from Diadone Research (Cedex, France). Sensor chip SA was obtained from BIAcore AB (Uppsala, Sweden).

Preparation of Octasaccharide Fractions from CDSNS-heparin and Heparin—One octasaccharide composed of HexA-$GlcNSO_3$ (Octa-I) and another composed of $HexA(2SO_4)$-$GlcNSO_3(6SO_4)$ (Octa-II) were prepared from CDSNS-heparin and heparin, respectively, as follows. One hundred milligrams of CDSNS-heparin was digested with 0.1 unit of heparitinase I, which is known to preferentially cleave glucosaminidic linkages to nonsulfated HexA residues in heparin/HS, at 37 °C for 2 h. The unsaturated oligosaccharide products were separated by Superdex 30 chromatography based on size. Octasaccharide fractions were pooled and lyophilized. The lyophilized materials were applied to a Mono Q column. The Mono Q column was developed by using a linear gradient from 0.2 to 1.2 M NaCl in 50 mM glycine-HCl, pH 3.0. The fractions eluted around 0.34 to 0.38 M NaCl were pooled and desalted by PD-10 column chromatography. The purified octasaccharide thus obtained was designated Octa-I. About 250 nmol (as HexA) of Octa-I was obtained. One hundred milligrams of heparin was digested with 0.1 unit of heparinase, which is known to cleave preferentially glucosaminidic linkages to 2-*O*-sulfated IdoUA in heparin/HS, at 37 °C for 2 h. Octa-II was purified from the heparin digests by the methods described above except that the fractions eluted over 1.0 M NaCl were pooled in the Mono Q chromatography. About 2.4 μmol (as HexA) of Octa-II was obtained. Aliquots of Octa-I and Octa-II were reduced with [^{3}H]$NaBH_4$ as described by Shively and Conrad (33). The specific activities of ^{3}H-labeled Octa-I and Octa-II were 1.5×10^4 and 1.2×10^4 dpm/nmol, respectively.

Preparation of O-Sulfated CDSNS-Heparin Octasaccharide with Recombinant HS2ST and HS6ST-1—The recombinant hHS2ST and hHS6ST-1 were prepared and purified as described previously (19). Briefly, FLAG-CMV2-hHS2ST or hHS6ST-1 was transfected into COS-7 cells. After 72 h, the recombinant fusion proteins were extracted from the cell layer with 10 mM Tris-HCl, pH 7.2, 0.5% (v/v) Triton X-100, 0.15 M NaCl, 20% glycerol, 10 mM $MgCl_2$, and 2 mM $CaCl_2$ and purified with an anti-FLAG M2 antibody-conjugated affinity column.

2-*O*-Sulfated Octa-I and 6-*O*-sulfated Octa-I were prepared as follows. For 2-*O*-sulfation of Octa-I, the reaction mixture contained, in a final volume of 50 μl, 1.0 μmol of acetate buffer, pH 5.5, 3.75 μg of protamine chloride, 0.5 nmol of Octa-I, 1 μCi/2 nmol of [^{35}S]PAPS, and 2.7 units of hHS2ST. For 6-*O*-sulfation, the reaction mixture (50 μl) contained 2.5 μmol of imidazole-HCl, pH 6.8, 3.75 μg of protamine chloride, 0.5 nmol of Octa-I, 2 nmol of [^{35}S]PAPS (1 μCi), and 5.5 units of hHS6ST-1. After incubation at 37 °C overnight, the reactions were stopped by heating at 100 °C for 1 min. 2-*O*-^{35}S-Sulfated Octa-I and 6-*O*-^{35}S-sulfated Octa-I were precipitated with 3 volumes of ethanol containing 1.3% potassium acetate and 0.5 mM EDTA in the presence of the carrier chondroitin 4-sulfate (0.1 μmol as glucuronic acid). The precipitates were dissolved in a small volume of distilled water and subjected to Mono Q chromatography. The Mono Q chromatography was developed with a linear gradient from 0.2 to 0.8 M in 50 mM glycine-HCl, pH 3.0.

Preparation of Growth and Differentiation Factor (HBGF)-conjugated Sepharose Gel—The growth and differentiation factor-conjugated Sepharose gel was prepared as described previously (30). Briefly, each of FGF-2 (50 μg), FGF-4 (50 μg), FGF-7 (100 μg), FGF-8 (50 μg), FGF-10 (100 μg), FGF-18 (100 μg), HGF (100 μg), BMP-6 (100 μg), and VEGF (50 μg) was coupled to 0.3 ml of CNBr-activated Sepharose 4B gel according to the method recommended by the manufacturer. Acetylated heparin (10 μg) was added to the coupling reaction mixture to protect the heparin/heparan sulfate-binding site of these growth factors.

HBGF Affinity Chromatography of Various Octasaccharides—0.1 nmol of ^{35}S-labeled octasaccharide was dissolved in 0.5 ml of PBST, 0.9 mM $CaCl_2$, and 0.2 mg/ml chondroitin 4-sulfate (Binding buffer) and applied to a syringe column of GF-Sepharose (0.3 ml) equilibrated with Binding buffer at 4 °C. The column was shaken gently for 1 h and then washed with 2.5 ml of PBS containing 0.9 mM $CaCl_2$ and 0.05% Tween 20 (PBST(+)). The column was eluted stepwise with 1 ml of 0.20, 0.25, 0.30, 0.35, 0.40, 0.45, and 0.50 M NaCl in PBST(+) and 2 ml of 2 M NaCl in PBS containing 0.05% Tween 20 (PBST) (Elution buffer). In some cases, the octasaccharides were eluted with 2 ml of Elution buffer after the wash with 2.5 ml of PBST(+). The elution profiles were monitored by measuring the radioactivity in a liquid scintillation counter (30).

Surface Plasmon Resonance Analysis—Real time analysis of the interaction of growth factors and heparin/modified heparin was performed with a BIAcore 2000 SPR biosensor. Streptavidin-conjugated Sensor Chip SA was used to immobilize various glycosaminoglycans. Glycosaminoglycans were biotinylated according to the method recommended by the manufacturer. Two hundred micrograms of heparin, 2ODS-heparin, 6ODS-heparin, or chondroitin 4-sulfate was incubated with 74 μg of NHS-LS-Biotin (Pierce) in 100 μl of 50 mM sodium bicarbonate buffer, pH 8.5, for 30 min at room temperature. Biotinylated glycosaminoglycans were precipitated with 2.5 volumes of 95% (v/v) ethanol containing 1.3% (w/v) potassium acetate, and the process was repeated three times. In order to immobilize GAGs on the sensor chip SA, 0.5–2 μg/ml biotinylated GAGs in PBST were injected at a flow rate of 5 μl/min. The injection of biotinylated GAGs produced 10–200 response units of immobilized GAG on the biosensor surface. The amount of bound material on the biosensor chips was measured in arbitrary response units. All measurements were carried out at room temperature, and refractive index errors due to bulk solvent effects were corrected by subtracting away responses on the non-coated sensor chip for GF concentrations used. Each GF stock solutions were diluted with PBST.

Various concentrations of growth factors were injected across the GAG-coated surface at a flow rate of 5 μl/min. The steady state binding level was monitored for 300 s. Sensorgrams were evaluated using BIAevaluation software. Dissociation constants (K_D) for binding could be extracted from the dependence of steady state binding levels on GF concentration. In a steady state, this model calculates K_D from a plot of R_{eq} against C according to the equation, $K_D = R_{eq}(R_{max} - R_{eq})/C$, where R_{eq} is the steady state response level for the growth factor; R_{max} is the maximal capacity of the sensor chip to bind growth factors expressed in response units; and C is the molar concentration of growth factor.

HBGF-releasing Activity of Octasaccharides from HS—The releasing

TABLE I
Disaccharide compositions of octasaccharides

The samples were digested with a mixture of heparitinase I and II and heparinase. The products were determined by a reversed-phase ion-pair chromatography with sensitive and specific postcolumn detection. ND, not detected.

	Octasaccharide library							
	Octa-I	Octa-II	2S-1	2S-2	2S-3	6S-1	6S-2	6S-3
	units/octasaccharide							
Disaccharide component								
HexA-GlcNAc	ND	0.1	ND	ND	ND	ND	ND	ND
HexA-GlcNS	4.0	0.1	2.9	1.9	1.1	2.9	1.9	1.2
HexA-GlcNAc(6S)	ND	0.1	ND	ND	ND	ND	ND	ND
HexA(2S)-GlcNS	ND	0.3	1.1	2.1	2.9	ND	ND	ND
HexA-GlcNS(6S)	ND	0.5	ND	ND	ND	1.1	2.1	2.8
HexA(2S)-GlcNS(6S)	ND	2.9	ND	ND	ND	ND	ND	ND
Yield (%)			40	16	6	38	20	8

activity was measured by ELISA as described previously with a minor modification (30). A 96-well streptavidin-coated plate (Thermo Labsystems, Finland) was coated with 0.1 nmol (as hexuronic acid) of biotinylated pig aorta HS for 1 h at room temperature. Wells were washed three times with 200 μl of PBS and then blocked with 200 μl of PBS containing 10 mg/ml BSA for 1 h with gentle shaking. Wells were washed three times with PBS. Then 100 μl of Binding buffer (see above) containing 40 ng/ml digoxigenin-conjugated HBGF and 10 mg/ml BSA was added into each well. After 1 h at room temperature, unbound digoxigenin-conjugated HBGF was removed by three washes with PBST(+). Then 100 μl of Binding buffer containing 10 mg/ml BSA and 1 pmol to 1 nmol of each octasaccharide were added into the wells. After 1 h at room temperature, wells were washed, and then alkaline phosphatase-conjugated Fab fragments of anti-digoxigenin antibody (1:1000 dilution) were added. After 1 h at room temperature, unbound Fab fragments were removed by three washes with PBST, and the alkaline phosphatase substrate (1 mg/ml *p*-nitrophenyl phosphate in 1 M diethanolamine, pH 9.8) was added into each well. The enzyme activity in each well was measured by using a microplate reader. The experiments were independently repeated three times, and statistical analyses were performed using Student's *t* test. The criterion of significance was shown by *p* values.

Compositional Analysis of Octasaccharides—About 0.3 nmol of octasaccharides was digested with a mixture of 1 milliunit of heparitinase I, 0.1 milliunit of heparitinase II, and 1 milliunit of heparinase in 50 μl of 50 mM Tris-HCl, pH 7.2, 1 mM $CaCl_2$, and 5 μg of BSA at 37 °C for 1 h. Unsaturated disaccharide products were analyzed by fluorometric postcolumn high performance liquid chromatography (HPLC) as reported previously (35).

RESULTS

Preparation of an Octasaccharide Library—Octa-I, an oligosaccharide composed of HexA-$GlcNSO_3$, and Octa-II, an oligosaccharide composed of HexA($2SO_4$)-$GlcNSO_3$($6SO_4$), were prepared from CDSNS-heparin and heparin, respectively, as described under "Experimental Procedures." The structures of these oligosaccharides were confirmed by digestion with a mixture of heparitinase and heparinase followed by HPLC analysis as described under "Experimental Procedures." As shown in Table I, ΔHexA-$GlcNSO_3$ was exclusively obtained from Octa-I, indicating that the structure of Octa-I was ΔHexA-$GlcNSO_3$-(HexA-$GlcNSO_3$)$_3$. On the other hand, 3 mol of HexA($2SO_4$)-$GlcNSO_3$($6SO_4$), 0.5 mol of HexA-$GlcNSO_3$($6SO_4$), and 0.5 mol of other disaccharide components were released from 1 mol of Octa-II. Octa-II was thus a mixture containing 3 units of HexA($2SO_4$)-$GlcNSO_3$($6SO_4$) per molecule.

2-*O*-Sulfated and 6-*O*-sulfated Octa-I were prepared by incubating Octa-I with the recombinant HS2ST and HS6ST-1, respectively, together with PAPS as described under "Experimental Procedures." The *in vitro* sulfated products were separated with Mono Q chromatography (Fig. 1). Both 2-*O*-sulfated Octa-I and 6-*O*-sulfated Octa-I were separated into three peaks: 2S-1, 2S-2, and 2S-3 for 2-*O*-sulfated Octa-I; and 6S-1, 6S-2, and 6S-3 for 6-*O*-sulfated Octa-I. All of these peaks were eluted at higher NaCl concentration than Octa-I and at lower NaCl concentration than Octa-II. Each peak was pooled separately. To examine the structure of these products, aliquots of these sulfated octasaccharides were digested extensively with the mixture of heparitinase and heparinase and subjected to HPLC as described under "Experimental Procedures." From the disaccharide compositions shown in Table I, it is evident that 2S-1, 2S-2, and 2S-3 contained 1, 2, and 3 units, respectively, of the HexA($2SO_4$)-$GlcNSO_3$ component; and 6S-1, 6S-2, and 6S-3 have 1, 2, and 3 units, respectively, of HexA-$GlcNSO_3$($6SO_4$) component. Under the maximum reaction conditions used, more than 60% of Octa-I was sulfated by each sulfotransferase. The yields of these sulfated Octa-I were decreased as the content of 2-*O*-sulfated or 6-*O*-sulfate units was increased (Table I).

Binding Abilities of Octa-I and Octa-II to Various HBGFs—Before determining the binding activity of oligosaccharides, we examined the binding ability and capacity of the growth and differentiation factor-conjugated Sepharose 4B affinity columns using ^{3}H-labeled heparin (2 nmol as HexA). Every affinity column conjugated with FGF-2, FGF-4, FGF-7, FGF-8, FGF-10, FGF-18, HGF, VEGF, or BMP-6 bound more than 80% of the applied ^{3}H-labeled heparin (data not shown). To examine the binding activity of the oligosaccharide libraries synthesized enzymatically, we first applied [^{3}H]$NaBH_4$-reduced Octa-II (0.5 nmol as octasaccharide) to the growth factor-conjugated columns. The amounts of Octa-II bound to various growth factor-conjugated columns are shown in Fig. 2. FGF-2, FGF-4, FGF-18, and HGF bound Octa-II strongly. FGF-10 and FGF-7 also bound Octa-II slightly weaker than FGF-2. In contrast, FGF-8, BMP-6, and VEGF hardly bound Octa-II (less than 15% of the applied). These results indicate that FGF-2, FGF-4, FGF-7, FGF-10, FGF-18, and HGF have high affinity to Octa-II as observed for heparin, but FGF-8, BMP-6, and VEGF have very weak or no affinity to Octa-II, although these proteins showed high affinity to heparin. The results suggest that oligosaccharides longer than octasaccharides may be required for the binding of FGF-8, BMP-6, or VEGF.

Octa-II contains both *O*-sulfate and *N*-sulfate. To address which sulfate groups are necessary for the binding to these growth factors, we examined the binding of Octa-I which is devoid of *O*-sulfate but has *N*-sulfate. As shown in Fig. 2, Octa-I hardly bound at all to the growth factor-conjugated affinity columns (*open bars* in Fig. 2). These results clearly indicate that the *O*-sulfate groups in Octa-II are essential for the binding to these growth factors.

Affinity of the Octasaccharide Library to Various HBGFs—Octa-II is composed of 3 units of HexA($2SO_4$)-$GlcNSO_3$($6SO_4$). To determine whether either or both of the 2-*O*-sulfate and 6-*O*-sulfate groups interact with the growth factors, we examined the binding of 2-*O*-sulfated or 6-*O*-sulfated Octa-I to the growth factor-conjugated columns that could retain Octa-II. In Fig. 3, the binding of 2S-3 and 6S-3 to FGF-2, FGF-4, FGF-7,

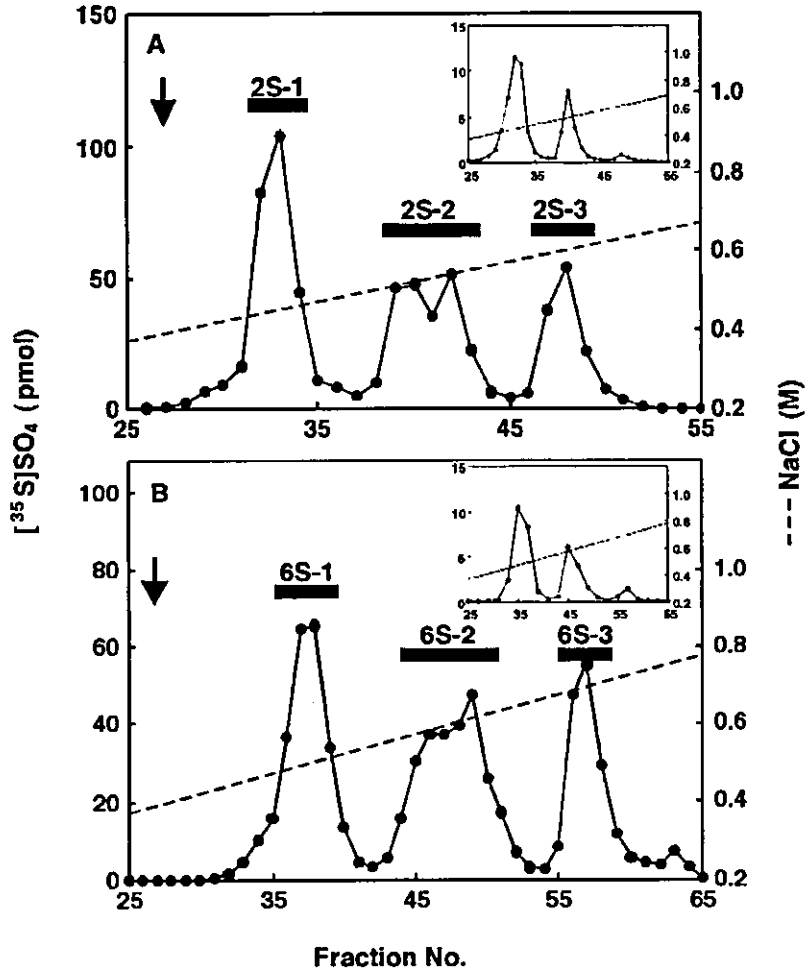

FIG. 1. **Mono Q column chromatography of 2-*O*-sulfated Octa-I and 6-*O*-sulfated Octa-I generated *in vitro* by recombinant enzymes.** 10 nmol of Octa-I was incubated with 20 μCi/40 nmol of [^{35}S]PAPS and recombinant human HS2ST or recombinant human HS6ST-1 overnight. 2-*O*-Sulfated Octa-I (*A*) and 6-*O*-sulfated Octa-I (*B*) were applied to a Mono Q column and eluted as described under "Experimental Procedures." Aliquots of fractions served for the measurements of radioactivity. The fractions shown by *solid horizontal bars* were pooled and desalted for analysis. *Broken lines* represent the concentration of NaCl. *Arrows* indicate the elution position of Octa-I. *Insets* show the elution profiles of the reaction products after the incubation for 90 min.

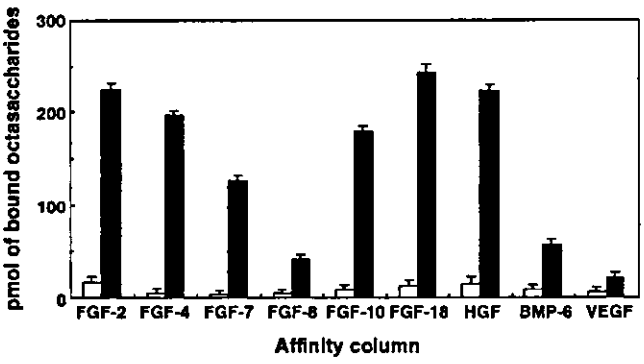

FIG. 2. **Binding of Octa-I and Octa-II to various growth and differentiation factors.** 500 pmol of ^{3}H-labeled Octa-I and Octa-II was applied to the GF affinity column as described under "Experimental Procedures." After incubation at 4 °C for 1 h, the column was washed with Binding buffer and then eluted with Elution buffer (bound fraction). *Open bars* and *closed bars* indicate amount of bound Octa-I and Octa-II, respectively.

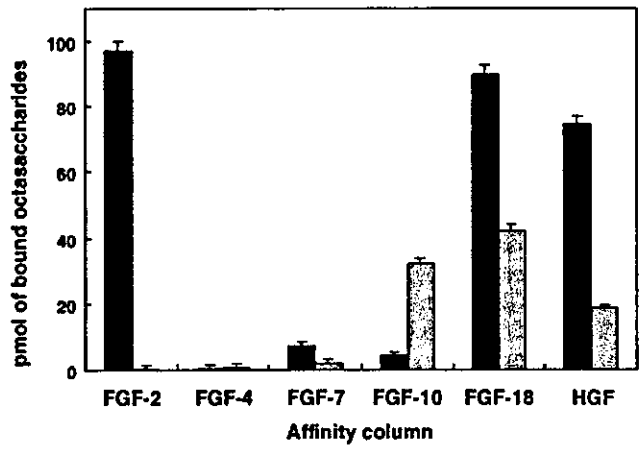

FIG. 3. **Binding of 2S-3 and 6S-3 to various growth and differentiation factors.** 100 pmol of octasaccharides "2S-3" and "6S-3" was subjected to the GF affinity column chromatography as described under "Experimental Procedures." After incubation at 4 °C for 1 h, the column was washed with Binding buffer and then eluted with Elution buffer (bound fraction). *Closed bars* and *gray bars* indicate amount of bound 2S-3 and 6S-3, respectively.

FGF-10, FGF-18, or HGF-conjugated columns is shown. FGF-2 bound 2S-3 strongly but did not bind 6S-3. These results are consistent with studies showing that the presence of 1 unit of the HexA(2SO$_4$)-GlcNSO$_3$ component in oligosaccharides is sufficient for the binding to FGF-2 (26, 27). In contrast, FGF-10 interacted moderately with 6S-3 but little with 2S-3. FGF-18 and HGF bound both 2S-3 and 6S-3, but preferred 2-*O*-sulfated to 6-*O*-sulfated octasaccharides. Because FGF-4 and FGF-7 bound neither 2S-3 nor 6S-3, these HBGFs appear to require trisulfated disaccharide units, IdoUA(2SO$_4$)- GlcNSO$_3$(6SO$_4$), for the binding of oligosaccharides. Alternatively, FGF-4 and FGF-7 may bind octasaccharides containing both IdoUA(2SO$_4$)-GlcNSO$_3$ and HexA-GlcNSO$_3$(6SO$_4$) units. These results suggest that each growth factor may recognize the characteristic sulfation pattern of the octasaccharides. Furthermore, we determined the effect of the number of sulfate groups attached to the octasaccharides on the binding to HBGFs using octasaccharides with one, two, or three 2-*O*-sulfate groups (2S-1, 2S-2, and 2S-3) and octasaccharides with

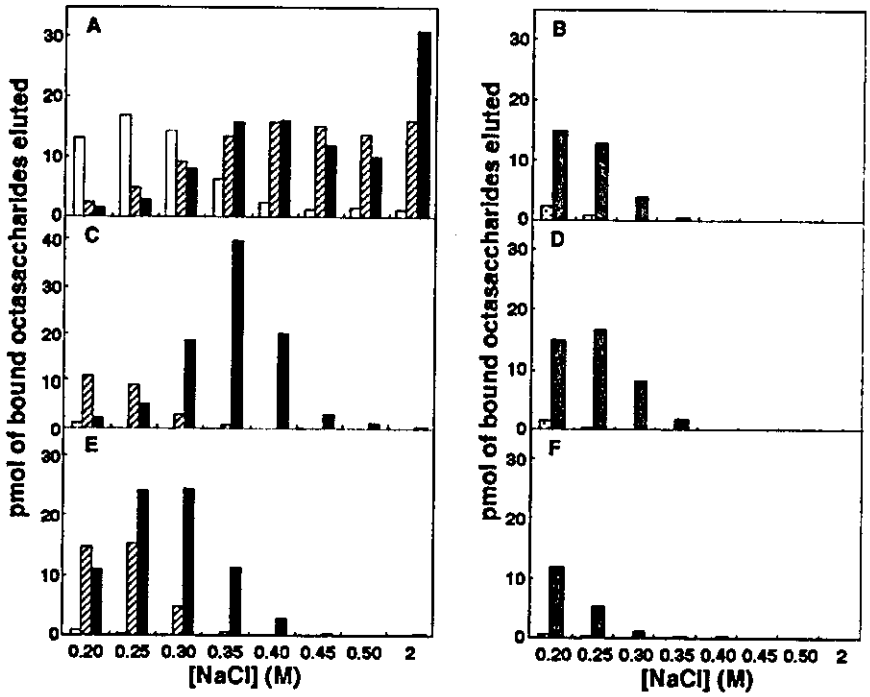

FIG. 4. **Affinity profiles of 2-*O*-sulfated or 6-*O*-sulfated octasaccharides for various growth and differentiation factors.** 100 pmol of octasaccharide was applied to GF affinity columns as described under "Experimental Procedures." After a wash with binding buffer, bound oligosaccharides were eluted with increasingly higher concentrations of NaCl. 2S-1 (*open bars*), 2S-2 (*striped bars*), and 2S-3 (*closed bars*) were subjected to FGF-2 (*A*), FGF-18 (*C*), and HGF (*E*) affinity chromatography. 6S-2 (*dotted bar*) and 6S-3 (*gray bar*) were subjected to FGF-10 (*B*), FGF-18 (*D*), and HGF (*F*) affinity chromatography. Each of the bars indicates the amount of eluted octasaccharide.

one, two, or three 6-*O*-sulfate groups (6S-1, 6S-2, and 6S-3). To the FGF-2-conjugated column, 57% of 2S-1 and more than 90% of 2S-2 and 2S-3 applied were bound. The majority of the bound 2S-1 was released by 0.35 M NaCl, but a complete release of 2S-2 and 2S-3 was attained with 2.0 M NaCl (Fig. 4*A*). These results indicate that the presence of only 1 unit of HexA($2SO_4$)-GlcNSO_3 is sufficient to retain the octasaccharides on FGF-2, and that the affinity of octasaccharides containing 2 or 3 units of HexA($2SO_4$)-GlcNSO_3 to FGF-2 is much higher than that of the other growth factors examined. To the FGF-10-conjugated column, 32% of 6S-3 was bound but neither 6S-2 nor 6S-1 was bound (Fig. 4*B*). These results suggest that 3 units of HexA-GlcNSO_3($6SO_4$) are required for the binding of 6-*O*-sulfated Octa-I to FGF-10. Because 48% of the bound 6S-3 was released by 0.25 M NaCl, the interaction of FGF-10 with 6-*O*-sulfated octasaccharides should be relatively weak. As observed in Fig. 3, FGF-18 and HGF showed affinity to both 2-*O*-sulfate and 6-*O*-sulfate, and the affinity to 2-*O*-sulfate seemed to be higher than to 6-*O*-sulfate. These results were confirmed by the binding experiments using different sulfated Octa-I molecules (Fig. 4). To the FGF-18-conjugated column, 90% of 2S-3, 42% of 6S-3, and 23% of 2S-2 were bound, but 6S-2, 6S-1, and 2S-1 were not bound. Quantitative elution of the bound 2S-3 and 6S-3 was achieved with 0.4 and 0.3 M, respectively, of NaCl (Fig. 4, *C* and *D*). Nearly the same results were obtained for the HGF-conjugated column (Fig. 4, *E* and *F*); 75% of 2S-3, 35% of 2S-2, and 19% of 6S-3 were bound, but 2S-1, 6S-2, and 6S-1 were not bound. Quantitative elution of the bound 2S-3 and 6S-3 was achieved with 0.35 and 0.25 M, respectively, of NaCl. However, a clear difference between FGF-18 and HGF was observed in the affinity to 6S-3; the affinity of HGF to 6S-3 was much lower than that of not only FGF-18 to 6S-3 but also HGF to 2S-2. These results indicate that FGF-18 and HGF require at least 2 units of HexA($2SO_4$)-GlcNSO_3 or 3 units of HexA-GlcNSO_3($6SO_4$) for the binding of the octasaccharides.

Analysis of the Interactions of $VEGF_{165}$ and BMP-6 with Modified Heparins Using Surface Plasmon Resonance Biosensor—As observed above, $VEGF_{165}$, BMP-6, and FGF-8 were able to bind heparin but did not bind Octa-II. To examine how 2-*O*-sulfate and 6-*O*-sulfate in heparin contributed to the binding to $VEGF_{165}$, BMP-6, and FGF-8, we determined the dissociation constant (K_D) between one of these HBGFs and intact 2-*O*-desulfated (2ODS) or 6-*O*-desulfated (6ODS) heparin. K_D values were determined by surface plasmon resonance (SPR) biosensor. As shown in Table II, 2-*O*-sulfate groups were completely removed from 2ODS-heparin, whereas a few 6-*O*-sulfate groups (up to 1.8%) remained in 6ODS-heparin. The major disaccharide components of heparin, 2ODS-heparin, and 6ODS-heparin were thus thought to be HexA($2SO_4$)-GlcNSO_3($6SO_4$), HexA-GlcNSO_3($6SO_4$), and HexA($2SO_4$)-GlcNSO_3, respectively. As positive controls, K_D values were also determined for FGF-2 and HGF. The K_D value observed in the system of FGF-2/heparin, FGF-2/2ODS-heparin, and FGF-2/6ODS-heparin was 23, 340, and 23 nM, respectively (Fig. 5, *A–C*, and Table III). Because the K_D for FGF-2/6ODS-heparin was the same as the K_D for FGF-2/heparin, the presence of 6-*O*-sulfated groups on GlcNSO_3 residues in heparin appeared to have no effect on the interaction between FGF-2 and heparin. In contrast, the K_D for FGF-2/2ODS-heparin was 15-fold that for FGF-2/heparin. In the case of HGF, the measured K_D for HGF/heparin, HGF/2ODS-heparin, and HGF/6ODS-heparin was 12, 86, and 58 nM, respectively (Fig. 5, *D–F*, and Table III). Both the K_D for HGF/2ODS-heparin and the K_D for HGF/6ODS-heparin were higher than the K_D values for HGF/heparin. These observed K_D values for the interactions of FGF-2 or HGF with the modified heparins are consistent with the results obtained from the octasaccharide library, and confirm the importance of 2-*O*-sulfate in the binding of FGF-2 and the importance of both 2-*O*- and 6-*O*-sulfate in the binding of HGF. Thus, the K_D values obtained by SPR biosensor using biotinylated glycosaminoglycans seem accurate enough to be compared quantitatively. Under the same conditions used for the interaction of FGF-2 and HGF, we determined K_D values for the interaction between $VEGF_{165}$ or BMP-6 and heparin or the modified ones. The measured K_D for $VEGF_{165}$/heparin, $VEGF_{165}$/2ODS-heparin, and $VEGF_{165}$/6ODS-heparin was 165, 524, and 592 nM, respectively (Fig. 5, *G–I*, and Table III). Both the K_D for $VEGF_{165}$/2ODS-heparin and the K_D for $VEGF_{165}$/6ODS-heparin were 3-fold the K_D values for $VEGF_{165}$/heparin. The measured K_D values for BMP-6/heparin, BMP-6/2ODS-heparin, and BMP-6/6ODS-heparin was 6.3, 11, and 15 nM, respectively (Fig. 5, *J–L*, and Table III), which indicate the

TABLE II
Disaccharide compositions of heparin and modified heparins

Disaccharide component	Heparin	2ODS-heparin	6ODS-heparin
	%	%	%
HexA-GlcNAc	5	6	7
HexA-GlcNS	1	12	10
HexA-GlcNAc(6S)	2	5	ND[a]
HexA(2S)-GlcNS	14	ND	75
HexA-GlcNS(6S)	7	77	6
HexA(2S)-GlcNS(6S)	71	ND	2

[a] ND, not detected.

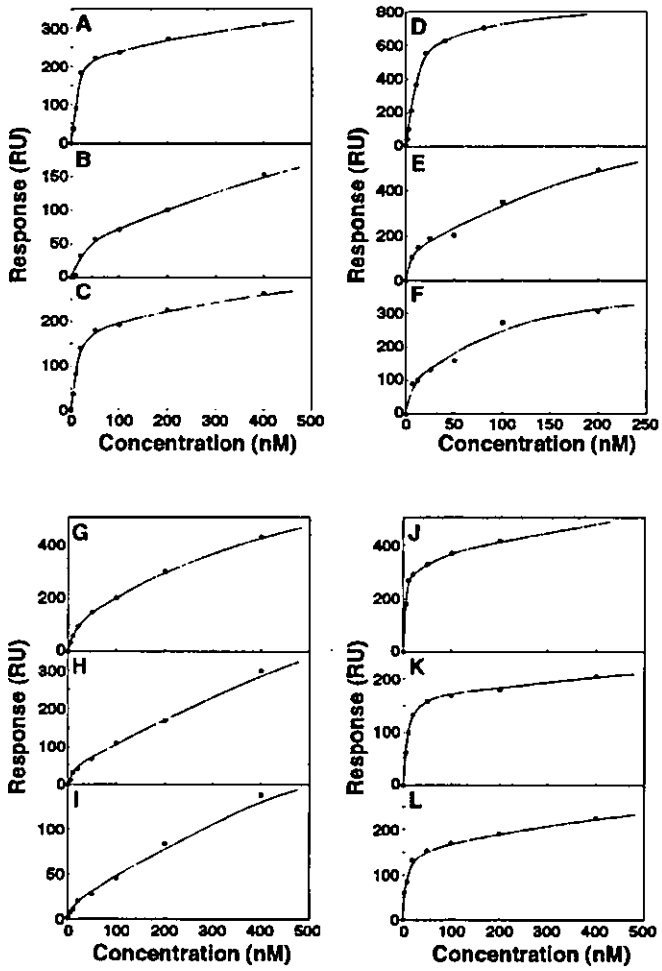

FIG. 5. **The response in steady state level plotted against the concentration of FGF-2, HGF, $VEGF_{165}$, and BMP-6.** Various concentrations of FGF-2 (*A–C*), HGF (*D–F*), $VEGF_{165}$ (*G–I*), and BMP-6 (*J–L*) were injected over the sensor tip-immobilized heparin (*A, D, G,* and *J*), 2ODS-heparin (*B, E, H,* and *K*), and 6ODS-heparin (*C, F, I,* and *L*). The response in the steady state was plotted against the concentration of each GF. The dissociation constant for the interaction was evaluated with these curves using BIA evaluation software.

TABLE III
Equilibrium dissociation constant for the interactions of FGF-2, HGF, $VEGF_{165}$, and BMP-6 with various chemically modified heparins
The K_D (nM) value was measured from Fig. 5.

Immobilized GAG	FGF-2	HGF	$VEGF_{165}$	BMP-6
Heparin	23	12	165	6.3
2ODS-heparin	340	86	524	11
6ODS-heparin	23	58	592	15

extremely high affinity of BMP-6 to heparin or the modified heparins. Even so, both the K_D for BMP-6/2ODS-heparin and the K_D for BMP-6/6ODS-heparin were 2- or 3-fold the K_D values for BMP-6/heparin. These results suggest that both 2-*O*-sulfate groups on HexA residues and 6-*O*-sulfate groups on $GlcNSO_3$ residues contained in heparin/HS are equally required for the interactions with $VEGF_{165}$ and BMP-6.

Because FGF-8 was bound nonspecifically to the sensor chips, the K_D values for FGF-8/modified heparins could not be determined. It should be of note here that no interactions between these growth factors and chondroitin 4-sulfate have been recognized (data not shown).

FGF-releasing Activity of Octasaccharide Library—As shown above, FGF-2 and FGF-10 bound the octasaccharides typically different from each other in that FGF-2 required 2-*O*-sulfate but FGF-10 needed 6-*O*-sulfate. Therefore, we examined whether the addition of 2-*O*-sulfated Octa-I and 6-*O*-sulfated Octa-I could release FGF-2 and FGF-10, respectively, from their complexes with pig aorta HS, which has the affinity for both FGF-2 and FGF-10 and is thought to represent natural HS in normal tissues. Streptavidin-coated ELISA plates were coated with the biotinylated HS. Digoxigenin-labeled FGF-2 or FGF-10 was then added to form complexes with the HS on plates. The incubation with various octasaccharides at different concentrations added to the plates released the digoxigenin-labeled FGF from the complexes, which was assessed by quantitating the labeled FGF left on the plates after several washes as described under "Experimental Procedures." The addition of 1 nmol/ml 6S-3 and 2S-3 released 29 and 8% of bound FGF-10, respectively (Fig. 6*A*), which corresponded to the releasing activity observed by the addition of 0.3 and 0.03 nmol/ml Octa-II, respectively (Fig. 6*B*), suggesting that 6S-3 is 10-fold more active in releasing FGF-10 than 2S-3. The addition of 1 nmol/ml Octa-II released 45% of bound FGF-10. Other *O*-sulfated Octa-I have none or only a slight effect on the releasing. In the case of the FGF-2 binding to the HS, the addition of 0.2 nmol/ml 2S-2, 2S-3, and Octa-II had almost the same releasing activity (57–61%), and that of 0.2 nmol/ml 2S-1 and 6S-3 released 26 and 11% of bound FGF-2, respectively (Fig. 6*C*), which corresponded to the releasing when 0.05 and 0.02 nmol/ml Octa-II were added, respectively (Fig. 6*D*). 2S-1 still showed 25% of the Octa-II activity although it had only one *O*-sulfate, but 6S-3 showed less than 10% of the Octa-II activity even though it had three *O*-sulfate residues. The observed differences of octasaccharide library in the releasing activity are good reflections of the differences in the binding specificity and activity of octasaccharide library to FGF-2 and FGF-10, which were described above.

DISCUSSION

We demonstrated that octasaccharide libraries composed of well defined sulfated octasaccharides generated by recombinant HS-*O*-sulfotransferases were useful for characterizing the binding structure for HBGFs. For FGF-2, FGF-4, FGF-7, FGF-8, FGF-10, FGF-18, HGF, BMP-6, and $VEGF_{165}$, we analyzed systematically the binding structures present in heparin/heparan sulfate, including the octasaccharide library. Based upon differences in affinity, these growth factors could be classified roughly into five groups. Group 1 had the affinity for 2-*O*-sulfated but not 6-*O*-sulfated octasaccharides (FGF-2). Group 2 had the affinity for 6-*O*-sulfated but not 2-*O*-sulfated octasaccharides (FGF-10). Group 3 had the affinity for both 2-*O*-sulfated and 6-*O*-sulfated octasaccharides but preferred 2-*O*-sulfated ones (FGF-18 and HGF). Group 4 required both 2-*O*-sulfate and 6-*O*-sulfate in octasaccharides for binding (FGF-4 and FGF-7). Group 5 hardly bound any octasaccharides significantly (FGF-8, BMP-6, and VEGF) (Fig. 7). The results indicate that the structural domain in heparin/heparan sulfate exhibiting affinity to each HBGF could be differentiated in terms of chain size, position to which the sulfate is attached,

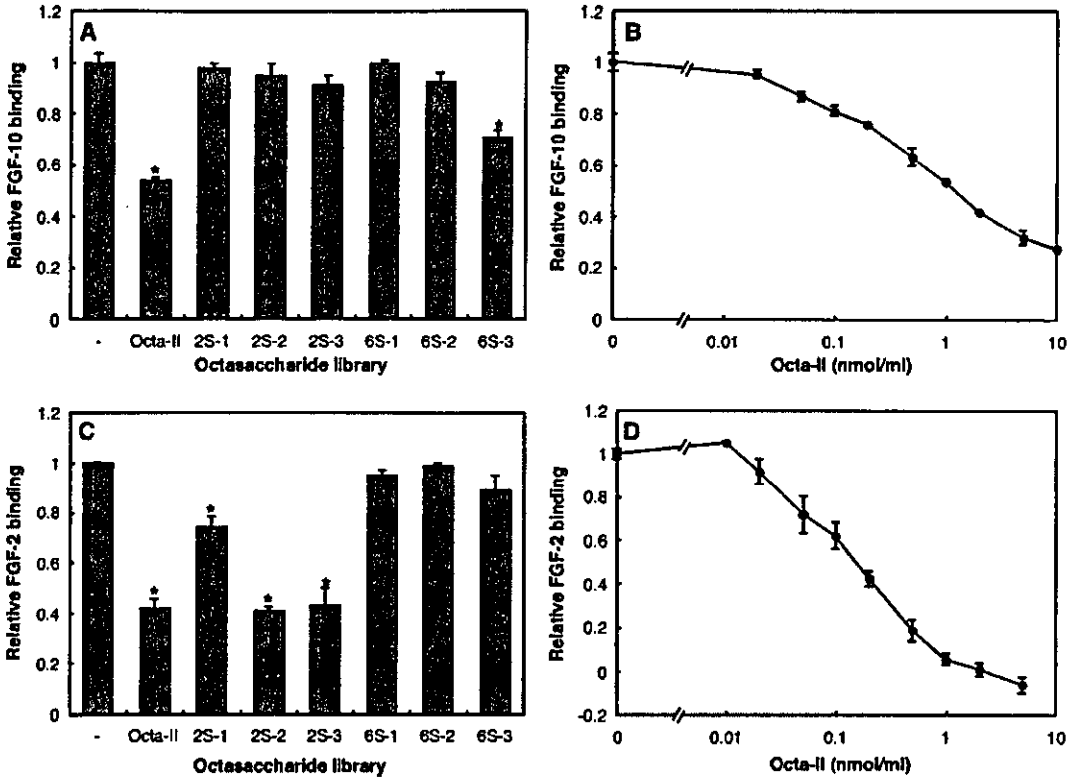

FIG. 6. **FGF-10 and FGF-2 releasing activity of octasaccharide library from the complex with HS.** Releasing activity was detected by ELISA as described under "Experimental Procedures." Digoxigenin-labeled FGF-10 (*A* and *B*) or FGF-2 (*C* and *D*) was added into wells coated with HS (0.1 nmol as hexuronic acid). After 1 h, unbound digoxigenin-labeled FGF was removed. Then 1 (*A*) and 0.2 nmol/ml (*C*) of octasaccharide library and Octa-II at various concentrations (*B* and *D*) were added. After 1 h, the wells were washed, and then anti-digoxigenin-AP, Fab fragments were added to yield color. Nonspecific binding was determined in the absence of FGFs. The experiments were independently repeated three times. The *columns* show mean values ± S.D. Statistical analyses were performed using Student's *t* test. Significance when compared with control was shown by the *asterisk* representing $p < 0.05$.

and the number and probably distribution of sulfate groups within the binding domain.

We also demonstrated relevance of the use of an octasaccharide library consisting of defined sulfated octasaccharides for characterizing the binding structures for HBGFs by their releasing activities of HBGFs from the complexes of HS and HBGFs. The affinity analyses using octasaccharide library revealed unique and almost opposite structural requirements for the bindings of FGF-10 and FGF-2. Therefore, we examined whether the addition of octasaccharides having the affinity to FGF-10 and FGF-2 could release FGF-10 and FGF-2, respectively, from their complexes with aorta HS. As expected from the affinity analyses, octasaccharides with the high affinity to FGF-10 or FGF-2 released specifically the respective FGF from their complexes with HS, and in addition, octasaccharides with the higher affinity gave the higher releasing activity (Fig. 6). These results suggest that the interactions of HS with certain HBGFs involved regions of the HS with specific sulfation patterns, and the exogenous addition or the endogenous generation of such regions as oligosaccharides may affect the bindings of HBGFs to HS and also to HBGF receptors. In the case of FGF, because HS is also known to bind to the growth factor receptors, the supply of HS oligosaccharides, whether it is exogenous or endogenous, may have some effect on their signaling. Further investigation remains on functions as the signaling regulators of these oligosaccharides.

Heparin-binding structures of the FGF family have been investigated by x-ray crystallographic analysis and biochemical analysis (36–38). From these studies, several basic amino acid residues were found to exist opposite the 2-*O*-sulfate group in heparin. Our results indicated that some members of the FGF family examined here had affinity to 2-*O*-sulfate, but FGF-10 exhibited little affinity to 2-*O*-sulfate. Instead, FGF-10 had affinity to the 6-*O*-sulfate group. To investigate whether the amino acid residues interacting with 2-*O*-sulfate groups are conserved in FGF-10, the putative heparin-binding region of FGF-10 was aligned with the same regions of other members of the FGF family having affinity to the 2-*O*-sulfate group (Fig. 7). It has been shown that the 2-*O*-sulfate-binding region of FGF-2 consists of Lys-125, Gln-134, Lys-135, and Ala-136 (39), whereas that of FGF-1 is composed of Asn-18, Lys-113, Lys-118, and Gln-127 (40) (see boldface amino acid residues in the partial amino acid sequences of FGF-2 and FGF-1 in Fig. 7). When the glycine boxes, which are commonly found in the FGF family and thought to correspond to motifs for heparin-binding sites, are aligned among FGF-2, FGF-4, FGF-7, FGF-8, FGF-10, and FGF-18, either Gln or Lys residues found in these putative 2-*O*-sulfate-binding sites are conserved in FGF-4, -7, -8, and -18 (see amino acid residues in the *gray boxes* in Fig. 7). However, these residues are not conserved in FGF-10 at all but are substituted for other amino acids. Crystallographic analysis of the FGF-10-heparin oligosaccharide complex will reveal the structure of the heparin-binding domain of FGF-10.

We demonstrated previously that the HGF-bound octasaccharide prepared from bovine liver HS contained 2 units of $IdoUA(2SO_4)$-$GlcNSO_3(6SO_4)$, whereas the HGF-unbound octasaccharide from the same HS contained only 1 unit of $IdoUA(2SO_4)$-$GlcNSO_3(6SO_4)$. On the other hand, Lyon *et al.* (29) reported that 2-*O*-sulfate groups contributed marginally to the interaction between HGF and fibroblast HS. Such an apparent discrepancy may be due partly to the difference in the heparan sulfate used. The present study clearly shows that HGF interacts with both 2-*O*-sulfate and 6-*O*-sulfate, because both the 2-*O*-sulfated octasaccharides containing 2 or 3 units of

Groups	(Necessary *O*-sulfate in octasaccharide)	GF		heparin binding regions of FGFs
				Glycine box
Group 1	(2-*O*-sulfate)	FGF-2	118 L	K R T G Q Y K L G S K T G P G Q K A I L
Group 2	(6-*O*-sulfate)	FGF-10	180 L	N G K G A P R R G Q K T R R K N T S A H
Group 3	(2-*O*- or 6-*O*-sulfate)	FGF-18	153 F	T K K G R P R K G P K T R E N Q Q D V H
		HGF		
Group 4	(2-*O*- and 6-*O*-sulfate)	FGF-4	181 L	S K N G K T K K G N R V S P T M K V T H
		FGF-7	167 L	N Q K G I P V R G K K T K K E Q K T A H
		(FGF-1)	111 L	K K N G S C K R G P R T H Y G Q K A I L
Group 5		FGF-8	171 F	T R K G R P R K G S K T R Q H Q R E V H
		VEGF		
		BMP-6		

FIG. 7. **Summary of *O*-sulfate essential for GF binding and comparison of heparin-binding regions in different FGFs.** The sequence alignment was performed using the ClustalW program (34, 36). All of the FGFs used in this alignment are from human. The sequences of the putative heparin-binding regions of FGFs that are structurally superimposed are shown, where the 2-*O*-sulfate-binding residues are indicated in *boldface*. *Square* shows glycine box, which is thought to correspond to motifs for heparin-binding sites (37).

HexA(2SO_4)-GlcNSO_3 and the 6-*O*-sulfated octasaccharides containing 3 units of HexA-GlcNSO_3(6SO_4) were bound to HGF. The fact that both 2-*O*-sulfate and 6-*O*-sulfate are involved in the interaction between HGF and HS was also supported by the crystallographic analysis of NK1 (a spliced variant of HGF)-heparin complexes. In this system, the 2-*O*-sulfate of HexA makes a hydrogen bond with Arg-73, whereas 6-*O*-sulfate of GlcNSO_3 makes a hydrogen bond with Lys-63 (41). In SPR analysis, the 2-*O*-desulfated heparin and 6-*O*-desulfated heparin prepared by region-selective desulfation dissociated faster from HGF than the native heparin (data not shown), supporting that both 2-*O*-sulfate groups in IdoUA and 6-*O*-sulfate groups in GlcNSO_3 play important roles in maintaining interaction with HGF.

We demonstrated that $VEGF_{165}$ did not bind octasaccharides with both 2-*O*- and 6-*O*-sulfate groups at all but bound the native heparin, indicating that $VEGF_{165}$ requires a longer binding domain than octasaccharide for binding heparin. Both 2-*O*-sulfate groups on HexA residues and 6-*O*-sulfate groups on GlcNSO_3 residues appear to contribute equally to the interaction between $VEGF_{165}$ and heparin, because the K_D value for $VEGF_{165}$/2ODS-heparin was nearly equal to the K_D value for $VEGF_{165}$/6ODS-heparin. Although the K_D value for $VEGF_{165}$/heparin was much larger than that for FGF-2/heparin or HGF/heparin, the interaction between $VEGF_{165}$ and heparin may still have relevance to some physiological processes, because the activity of $VEGF_{165}$ was stimulated *in vitro* by heparin, and mutant mice expressing only $VEGF_{121}$ lacking the heparin-binding domain showed abnormalities of microvascularization. Four spliced variants of VEGF, $VEGF_{145}$, $VEGF_{165}$, $VEGF_{189}$, and $VEGF_{206}$, may thus have important physiological functions through the interaction with HS. It remains to be studied what structures in HS could interact with the spliced variants other than $VEGF_{165}$ and how strong binding activity is.

To our knowledge, the direct interaction between BMPs and heparan sulfate has never been studied. However, there are a number of reports to suggest important roles of the interaction in differentiation and morphogenesis. For example, glypican-3, one of a family of six cell surface heparan sulfate proteoglycans in vertebrates, plays an important role in BMP signaling during limb patterning and skeletal development (42) and renal branching morphogenesis (43). The interaction of Dally, a glypican homolog, and Decapentaplegic, a TGF-β/BMP homolog, in *Drosophila* functions in the gradient formation of Decapentaplegic as a morphogen necessary for the wing and sensory organ formation (44–46). In the present study, we have shown that BMP-6 did not bind any octasaccharide, but by SPR analysis it bound heparin and 2ODS- or 6ODS-heparin with conspicuously high affinity. Chondroitin sulfate and CDSNS-heparin were a very poor ligand (data not shown). Therefore, the interaction with heparan sulfate should be very strong if the *O*-sulfated region is long enough. It is known that inducing activities of some members of the BMP family are tightly restricted to the region around the cells that produce them (47). Therefore, the observed high affinity of BMP-6 in the binding to HS likely reflects a role of HS in trapping the BMP. Because there are a number of the BMP family molecules with different activities (48), the present study raises an interesting question how each of them interacts with HS.

In our study Octa-II, octasaccharide containing three HexA(2SO_4)-GlcNSO_3(6SO_4) units derived from heparinase-digested heparin did not have the affinity enough to bind to FGF-8-conjugated column under the used conditions (Fig. 2). Because heparin was almost retained to this column, we judged FGF-8 needed the longer size for the binding. However, the minimal saccharide domain for the binding of FGF-8b, a spliced variant of FGF-8, has been reported to encompass 5–7 monosaccharide units of heparin (28). The observed discrepancy might have been caused by our usage of FGF-8, which is not a spliced variant, by some alteration in binding properties such as partial denaturation of our FGF-8 or by the difference in the reducing and nonreducing ends of oligosaccharide structures due to the preparation methods between ours (heparinase digestion) and theirs (nitrous acid degradation).

We prepared sulfated octasaccharides using the recombinant HS2ST and HS6ST-1. Up to 3 units of 2-*O*-sulfate could be introduced to the acceptor octasaccharide under the reaction conditions used here. Three units of 2-*O*-sulfate are probably the upper limit of sulfation, because unsaturated uronic acid at the nonreducing end of Octa-I could not be sulfated. When 60% of the acceptor substrate was converted to the 2-*O*-sulfated products, the octasaccharide having 1–3 units of 2-*O*-sulfate

was obtained at a ratio of 1.0:0.40:0.15. The one having 1 unit of 2-*O*-sulfate was a major product at the beginning of the reaction (Fig. 1, *insets*). It is thus unlikely that the sulfated octasaccharides behave better as an acceptor for HS2ST than the nonsulfated octasaccharide. As observed in the products of HS6ST-1, 6-*O*-sulfated Octa-I also separated into three major peaks; the octasaccharides with 1 unit of 6-*O*-sulfate were obtained in the highest yield even at the end of the reaction. HS6ST-1 appears to prefer nonsulfated octasaccharide as well. A small peak was observed after 6S-3 in the Mono Q chromatography. This peak may be an octasaccharide with 4 units of 6-*O*-sulfate groups, although the disaccharide composition of this peak has yet to be determined. It is of interest to examine the order and extent of 6-*O*-sulfation with HS6ST-1.

There are now a number of studies to demonstrate that HS is important to activate the growth factor binding to its receptor via the complex formation among them (5, 9), and longer HS oligosaccharides such as decasaccharides are involved in those interactions (25). Therefore, it is becoming important to generate oligosaccharide library of various sizes. In this regard, our present study may be the initial step for such a future study.

In conclusion, our approach using an octasaccharide library prepared *in vitro* appears to be useful for defining the specific structures required for binding various heparin-binding proteins. Furthermore, more divergent oligosaccharide libraries will be generated by the combined use of various HS modification enzymes such as other HS6ST isoforms and acceptor oligosaccharides of various sizes, and these oligosaccharides may allow more selective regulation of growth factor activities (see "Addendum"). In fact, the potential of such oligosaccharide libraries, containing mixed 2-*O*- and 6-*O*-sulfate substituents, has been demonstrated recently in analysis of sequence requirements for saccharides interacting with FGF-1 and FGF-2 (50).

Acknowledgments—We thank Drs. Hidenao Toyoda and Toshihiko Toida and Prof. Toshio Imanari (Faculty of Pharmaceutical Sciences, Chiba University, Chiba, Japan) for setting up a reversed-phase ion-pair chromatography system with sensitive and specific postcolumn detection. We also thank Prof. Ulf Lidahl (Department of Medical Biochemistry and Microbiology, Uppsala University, The Biomedical Center, Uppsala, Sweden) for exchanging the recent information on HS octasaccharide library and for useful discussions.

Addendum—During the review process of this manuscript, we reviewed the recent paper by Allen and Rapraeger (49) describing that HS structural requirements distinct from those for FGF binding are identified for both complex formation and signaling for each FGF and FGF receptor pair, which suggests the usefulness of the HS oligosaccharide library with longer chain sizes which we are going to generate.

REFERENCES

1. Conrad, H. E. (1998) *Heparin-Binding Proteins*, pp. 1–60, Academic Press, Inc., New York
2. David, G. (1993) *FASEB J.* **7**, 1023–1030
3. Yanagishita, M., and Hascall, V. C. (1992) *J. Biol. Chem.* **267**, 9451–9454
4. Aviezer, D., Hecht, D., Safran, M., Eisinger, M., David, G., and Yayon, A. (1994) *Cell* **79**, 1005–1013
5. Bernfield, M., Gotte, M., Park, P. W., Reizes, O., Fitzgerald, M. L., Lincecum, J., and Zako, M. (1999) *Annu. Rev. Biochem.* **68**, 729–777
6. Folkman, J., Klagsbrun, M., Sasse, J., Wadzinski, M., Ingber, D., and Vlodavsky, I. (1988) *Am. J. Pathol.* **130**, 393–400
7. Kjellen, L., and Lindahl, U. (1991) *Annu. Rev. Cell Biol.* **60**, 443–475
8. Rapraeger, A. C. (1993) *Curr. Opin. Cell Biol.* **5**, 844–853
9. Nakato, H., and Kimata, K. (2002) *Biochim. Biophys. Acta* **1573**, 312–318
10. Grobe, K., Ledin, J., Ringvall, M., Holmborn, K., Forsberg, E., Esko, J. D., and Kjellen, L. (2002) *Biochim. Biophys. Acta* **1573**, 209–215
11. HajMohammadi, S., Enjyoji, K., Princivalle, M., Christi, P., Lech, M., Beeler, D., Rayburn, H., Schwartz, J. J., Barzegar, S., de Agostini, A. I., Post, M. J., Rosenberg, R. D., and Shworak, N. W. (2003) *J. Clin. Investig.* **111**, 989–999
12. Bullock, S. L., Fletcher, J. M., Beddington, R. S., and Wilson, V. A. (1998) *Genes Dev.* **12**, 1894–1906
13. Orellana, A., Hirschberg, C. B., Wei, Z., Swiedler, S. J., and Ishihara, M. (1994) *J. Biol. Chem.* **269**, 2270–2276
14. Eriksson, I., Sandback, D., Ek, B., Lindahl, U., and Kjellen, L. (1994) *J. Biol. Chem.* **269**, 10438–10443
15. Aikawa, J., and Esko, J. D. (1999) *J. Biol. Chem.* **274**, 2690–2695
16. Aikawa, J., Grobe, K., Tsujimoto, M., and Esko, J. D. (2001) *J. Biol. Chem.* **276**, 5876–5882
17. Li, J.-P., Hagner-McWhirter, A., Kjellen, L., Jaan Palgi, M. J., and Lindahl, U. (1997) *J. Biol. Chem.* **272**, 28158–28163
18. Kobayashi, M., Habuchi, H., Yoneda, M., Habuchi, O., and Kimata, K. (1997) *J. Biol. Chem.* **272**, 13980–13985
19. Habuchi, H., Kobayashi, M., and Kimata, K. (1998) *J. Biol. Chem.* **273**, 9208–9213
20. Habuchi, H., Tanaka, M., Habuchi, O., Yoshida, K., Suzuki, H., Ban, K., and Kimata, K. (2000) *J. Biol. Chem.* **275**, 2859–2868
21. Liu, J., Shworak, N. W., Sinay, P., Schwartz, J. J., Zhang, L., Fritze, L. M., and Rosenberg, R. D. (1999) *J. Biol. Chem.* **274**, 5185–5192
22. Shworak, N. W., Liu, J., Petros, L. M., Zhang, L., Kobayashi, M., Copeland, N. G., Jenkins, N. A., Rosenberg, R. D., Eriksson, I., Sandback, D., Ek, B., Lindahl, U., and Kjellen, L. (1999) *J. Biol. Chem.* **274**, 5170–5184
23. Turnbull, J. E., Fernig, D. G., Ke, Y., Wilkinson, M. C., and Gallagher, J. T. (1992) *J. Biol. Chem.* **267**, 10337–10341
24. Habuchi, H., Suzuki, S., Saito, T., Tamura, T., Harada, T., Yoshida, K., and Kimata, K. (1992) *Biochem. J.* **285**, 805–813
25. Guimond, S., Maccarana, M., Olwin, B. B., Lindahl, U., and Rapraeger, A. C. (1993) *J. Biol. Chem.* **268**, 23906–23914
26. Ishihara, M. (1994) *Glycobiology* **4**, 817–824
27. Kreuger, J., Salmivirta, M., Sturiale, L., Gimenez-Gallego, G., and Lindahl, U. (2001) *J. Biol. Chem.* **276**, 30744–30752
28. Loo, B. M., and Salmivirta, M. (2002) *J. Biol. Chem.* **277**, 32616–32623
29. Lyon, M., Deakin, J. A., Mizuno, K., Nakamura, T., and Gallagher, J. T. (1994) *J. Biol. Chem.* **269**, 11216–11223
30. Ashikari, S., Habuchi, H., and Kimata, K. (1995) *J. Biol. Chem.* **270**, 29586–29593
31. Deakin, J. A., and Lyon, M. (1999) *J. Cell Sci.* **112**, 1999–2009
32. Feyzi, E., Lustig, F., Fager, G., Spillmann, D., Lindahl, U., and Salminirta, M. (1997) *J. Biol. Chem.* **272**, 5518–5524
33. Shively, J. E., and Conrad, H. E. (1976) *Biochemistry* **15**, 3932–3942
34. Thompson, J. D., Higgins, D. G., and Gibson, T. J. (1994) *Nucleic Acids Res.* **22**, 4673–4680
35. Toyoda, H., Kinoshita-Toyoda, A., and Selleck, S. B. (2000) *J. Biol. Chem.* **275**, 2269–2275
36. Plotnikov, A. N., Hubbard, S. R., Schlessinger, J., and Mohammadi, M. (2000) *Cell* **101**, 413–424
37. Luo, Y., Lu, W., Mohamedali, K. A., Jang, J. H., Jones, R. B., Gabriel, J. L., Kan, M., and McKeehan, W. L. (1998) *Biochemistry* **37**, 16506–16515
38. Raman, R., Venkataraman, G., Ernst, S., Sasisekharan, V., and Sasisekharan, R. (2003) *Proc. Natl. Acad. Sci. U. S. A.* **100**, 2357–2362
39. Faham, S., Hileman, R. E., Fromm, J. R., Linhardt, R. J., and Reed, D. C. (1996) *Science* **271**, 1116–1120
40. DiGabriele, A. D., Lax, I., Chen, D. I., Svahn, C. M., Jaye, M., Schlessinger, J., and Hendrickson, W. A. (1998) *Nature* **393**, 812–817
41. Lietha, D., Chirgadze, D. Y., Mulloy, B., Blundell, T. L., Gherardi, E., Ohuchi, H., Yoshioka, H., Tanaka, A., Kawakami, Y., Nohno, T., Noji, S., Shworak, N. W., Liu, J., Petros, L. M., Zhang, L., Kobayashi, M., Copeland, N. G., Jenkins, N. A., Rosenberg, R. D., Eriksson, I., Sandback, D., Ek, B., Lindahl, U., and Kjellen, L. (2001) *EMBO J.* **20**, 5543–5555
42. Paine-Saunders, S., Viviano, B. L., Zupicich, J., Skarnes, W. C., and Saunders, S. (2000) *Dev. Biol.* **225**, 179–187
43. Grisaru, S., Cano-Gauci, D., Tee, J., Filmus, J., and Rosenblum, N. D. (2001) *Dev. Biol.* **231**, 31–46
44. Fujise, M., Takeo, S., Kamimura, K., Matsuo, T., Aigaki, T., Izumi, S., and Nakato, H. (2003) *Development* **130**, 1515–1522
45. Fujise, M., Izumi, S., Selleck, S. B., and Nakato, H. (2001) *Dev. Biol.* **235**, 433–448
46. Selleck, S. B. (2000) *Trends Genet.* **16**, 206–212
47. Ohkawara, B., Iemura, S., ten Dijke, P., and Ueno, N. (2002) *Curr. Biol.* **12**, 205–209
48. Reddi, A. H. (1998) *Nat. Biotechnol.* **16**, 247–252
49. Allen, B. L., and Rapraeger, A. C. (2003) *J. Cell Biol.* **163**, 637–648
50. Jemth, P., Kreuger, J., Kusche-Gullberg, M., Sturiale, L., Gimenez-Gallego, G., and Lindahl, U. (2002) *J. Biol. Chem.* **277**, 30567–30573

Materials Transactions, Vol. 45, No. 4 (2004) pp. 989 to 993
Special Issue on Frontiers of Smart Biomaterials

Bonelike Apatite Coating on Skeleton of Poly(lactic acid) Composite Sponge

Hirotaka Maeda*[1], Toshihiro Kasuga*[2] and Masayuki Nogami

Graduate School of Engineering, Nagoya Institute of Technology, Nagoya 466-8555, Japan

A novel sponge, coated with bonelike apatite (b-HA) on its skeleton surface, was prepared using a particle-leaching technique combined with a biomimetic processing. A powder mixture consisting of calcium carbonate/poly(lactic acid) composite (CCPC) and sucrose was hot-pressed and then the resulting compact was soaked in the simulated body fluid at 37°C. Within the first hour, the sucrose was completely dissolved out, resulting in the formation of large-sized pores in the compact, and subsequently, after 3 hours of soaking, b-HA formed on the skeleton consisting of CCPC. On the other hand, on a pore-free CCPC, the apatite started to form after 12~18 hours. The induction period for b-HA formation on the skeleton of the CCPC sponge prepared using a particle-leaching technique is significantly shorter than that of the pore-free CCPC. The short period is suggested to originate from that a large amount of Ca^{2+} ion is rapidly supplied into the compartment space (pore) from the CCPC skeleton. The formed sponge has numerous, large pores of 450~580 μm in diameter, which are connected with channels having a diameter in the range of 70~120 μm, as well as a high porosity of 75%. Animal test using rats showed that the sponge has osteoconduction. The sponge is expected to be one of the promising candidates for osteoconducting fillers or tissue-engineering scaffolds.

(Received October 20, 2003; Accepted December 19, 2003)

Keywords: *bonelike apatite, sponge, poly(lactic acid), calcium carbonate, simulated body fluid, osteoconduction*

1. Introduction

Engineering living tissue for reconstructive surgery requires an appropriate cell source, optimal culture conditions, and a biodegradable scaffold as the basic elements. A scaffolding material is used either to induce formation of bone from the surrounding tissue or to act as a carrier or template for implanted bone cells or other agents. To serve as a scaffold, the material must be biocompatible, osteoconductive, and have a macroporous structure. Calcium phosphate ceramics such as hydroxyapatite or tricalcium phosphate, which have a osteoconductivity, were reported to be applied to scaffolds for bone tissue engineering.[1–3)]

Recently, much attention has been paid to bonelike hydroxycarbonate apatite (b-HA) as a novel biomaterial, since b-HA is very similar to the apatite in terms of living bone in its chemical composition and structure[4)] and shows effective compatibility in cell attachment, proliferation, and differentiation on the material,[5)] *i.e.*, osteoconductivity, as well as good bioresorbability.[6)] We expect that the sponges composed of b-HA skeleton can be applied to bone-fillers or scaffolds for tissue engineering. However, in general, ceramics have brittleness and low resistance against an impact loading. Such ceramic sponge materials have a serious risk to be broken in normal handling during operations. To eliminate this risk, it has been reported that the composites were fabricated using the polymer sponge coated with bioactive materials such as hydroxyapatite or Bioglass.[7–9)]

We reported earlier that a compact of calcium carbonate (vaterite)/poly(lactic acid) composite (CCPC) was reported to form b-HA on its surface even after 3 hours of soaking in SBF at 37°C.[10)] The rapid formation of the b-HA was suggested to originate from the integration of PLA having carboxy groups bonded with Ca^{2+} ions for b-HA nucleation and a large amount of calcium carbonate (vaterite) having an ability to effectively increase the supersaturation of b-HA due to the fast dissolution of the nano-sized vaterite. We believe that various novel biomaterials can be prepared using CCPC.

In the present work we biomimetically prepared the novel sponge composed of PLA composite skeleton coated with b-HA utilizing CCPC for applications to osteoconducting, bioresorbable bone-fillers or tissue engineering scaffolds.

2. Experimental Procedure

We have already reported that the CCPC containing ~30% calcium carbonate has an excellent mechanical properties with a high HCA-forming ability in SBF.[11)] The composite containing 30% calcium carbonate shows bending strength of 40~55 MPa, Young's modulus of 3.5~6 GPa, and significant ductility. In the present work the weight ratio of $CaCO_3$/PLA was determined to be 1/2.

Calcium carbonates consisting of vaterite were prepared by a carbonation process in methanol.[12)] CO_2 gas was blown for 3 hours at a flow rate of 300 mL/min into the suspension consisting of 7.0 g of $Ca(OH)_2$ in 180 mL of methanol at 0°C in a Pyrex® beaker. The resultant slurry was dried at 70°C in air, resulting in fine-sized powders. 2.0 g of PLA (with a molecular weight of 160 ± 20 kDa, determined by gel permeation chromatography) was dissolved in 20 mL of methylene chloride at room temperature. The calcium carbonate powders were added to the PLA solution and then the mixture was stirred to prepare a PLA slurry including the calcium carbonate powders.

The sponge was prepared using a conventional particle-leaching technique. In the present work sucrose was used as a sacrificial phase. Sucrose particles, which were sieved with the opening from 0.5~1.0 mm, were added to the PLA slurry. The nominal weight ratio of CCPC/sucrose was 1/6. The slurry mixture was stirred and then cast into a stainless steel die, and subsequently dried in air for solidification. After that, the product in the die was heated at 180°C and uniaxially hot-pressed at the temperature under a pressure of 40 MPa to

*[1]Graduate Student, Nagoya Institute of Technology
*[2]Corresponding author, E-mail: kasuga.toshihiro@nitech.ac.jp

prepare a CCPC/sucrose composite (denoted by sample A). After the hot-pressing, the specimen was cut in methanol with a diamond saw.

The hot-pressed sample was soaked in SBF (consisting of 2.5 mM of Ca^{2+}, 142.0 mM of Na^{+}, 1.5 mM of Mg^{2+}, 5.0 mM of K^{+}, 148.8 mM of Cl^{-}, 4.2 mM of HCO_3^{-}, 1.0 mM of HPO_4^{2-}, and 0.5 mM of SO_4^{2-}) that included 50 mM of $(CH_2OH)_3CNH_2$ and 45.0 mM of HCl at pH 7.4 at 37°C. After soaking, the sample was removed from SBF, gently washed with distilled water, and dried at room temperature. Our strategy for the preparation of the sponge composed of CCPC skeleton coated with b-HA is to leach out the sucrose phase and simultaneously to form b-HA on the composite skeleton.

The crystalline phases in the sponge were identified by X-ray diffraction analysis (XRD). The morphology of the sponge was observed by scanning electron microscopy (SEM). The pore size distribution of the sponge was measured by mercury porosimetry. The compressive strength of the sponge (7 mm × 7 mm × 10 mm) prepared by soaking in SBF for 3 days was estimated by a compressing test at a loading rate of 1 mm/min. Concentrations of Ca^{2+} and P^{5+} ions after soaking sample (10 mm × 10 mm × 5 mm) in SBF were determined by inductively coupled plasma atomic emission spectroscopy (ICP-AES). A compact of CCPC containing no sucrose powders (denoted by sample B), with the composition of $CaCO_3$/PLA = 1/2 in weight ratio, was used as a control material to compare with sample A (sponge).

The sponge (2-mm diameter × 10-mm thickness) prepared by soaking in SBF for 3 days was implanted into a femur of a 12-week-old Wister rat (male, weight; 265~285 g). The sponge was harvested and used for histological analysis at 4 weeks after implantation. The specimen was fixed, decalcified, embedded in paraffin, and stained with hematoxylin and eosin (HE). The specimen was observed with optical microscope.

3. Results & Discussion

Figure 1 shows XRD patterns before and after soaking the compact of CCPC/sucrose mixture in SBF. The XRD pattern before soaking shows that the hot-pressed compact consists of crystalline phases such as PLA, vaterite, aragonite and sucrose. After 1 hour of soaking, the peaks corresponding to sucrose and vaterite disappear; those to PLA and aragonite are seen. Sucrose was found to be completely dissolved even after 1 hour of soaking, resulting in formation of a sponge consisting of PLA and aragonite crystals. After 1 day of soaking, an additional broad peak at around $2\theta \sim 32°$, due to b-HA, is seen with the peaks due to PLA and aragonite.

Figure 2 shows the SEM photographs of the sample after 3 days of soaking in SBF. The SEM photograph shows that the sponge has numerous, large pores of 450~580 μm in diameter and large interconnected channels of 70~120 μm. The sponge has continuous open foams with a 3D interpenetrating network of struts and pores. As shown in Fig. 2(b), the surface of the CCPC skeleton is covered with the numerous deposits, that is b-HA, judged from the XRD pattern and the morphology. Further experiments showed

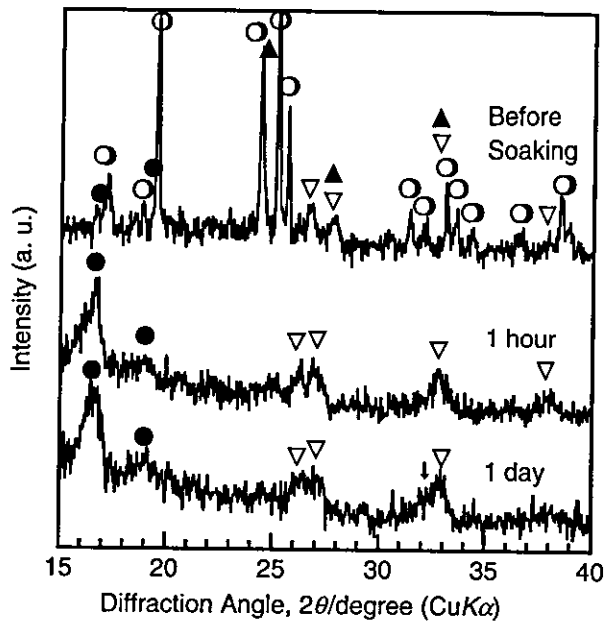

Fig. 1 XRD patterns of before and after soaking the compact of CCPC/sucrose mixture in SBF. (○) sucrose, (▲) vaterite, (▽) aragonite, (●) PLA, and (↓) apatite.

that apatite formation starts to occur after 3 hours of soaking.

Figure 3 shows the pore size distribution of the sponge prepared by soaking in SBF for 3 days. The median pore size of the sponge is 125 μm. There exist almost no pores below several tens micrometers in diameter. When a compact of the powder-mixture consisting of CCPC and sucrose was hot-pressed at 180°C, the sucrose particles melted (it begins to melt at 160°C), leading to adjacent particles connected each other. As a result, both the sucrose and CCPC phases were unified into an interconnecting three-dimensional network. The porosity was estimated from the measurement to be ~75%. The macroporous structure of the sponge prepared using sucrose may be likely to allow the migration of cells into the interior of the sponge. On the other hand, for comparison, when the sponge was prepared using sodium chloride, which were sieved with the opening from 0.5 to 1.0 mm, the median pore size in the sponge was estimated to be 65 μm. There exist numerous pores several tens micrometers in diameter. Since no sodium chloride melts during hot-pressed at 180°C, large-sized, interconnected particles as the sacrificial phase would not form.

In order to investigate apatite formation on CCPC in SBF after dissolution of the sucrose particles, the thicknesses of b-HA particles formed in SBF on the skeleton of sample A (the sponge derived from the compact of CCPC/sucrose mixture) and sample B were measured from cross-sectional SEM observation of their fracture face. The skeleton surface of sample A (sponge) was covered with numerous b-HA deposits after 3 hours of soaking (Fig. 2(b)). The b-HA formation did not occur within 2 hours. On the other hand, the surface of sample B was completely covered with b-HA after 18 hours of soaking. No b-HA formed on sample B within 12 hours. Figure 4 shows the thicknesses of b-HA layers formed on the skeleton surface of sample A or the surface of sample B as a function of the soaking time in SBF. The thickness of

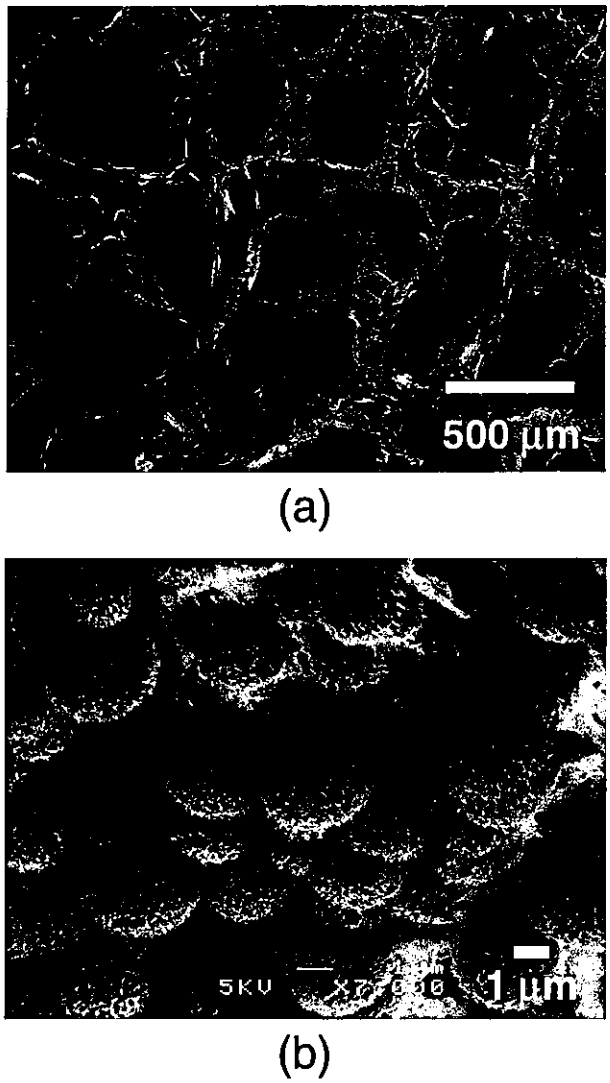

Fig. 2 SEM photographs of the sponge prepared by soaking in SBF for 3 hours. (a) cut surface of the sponge and (b) the magnified image of the skeleton surface.

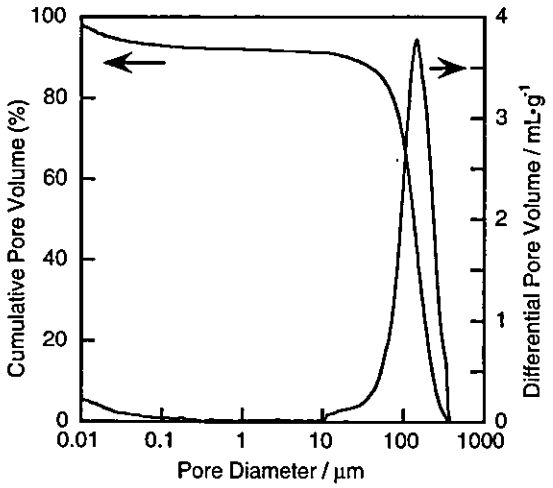

Fig. 3 Pore size distribution of the sponge prepared by soaking in SBF for 3 days.

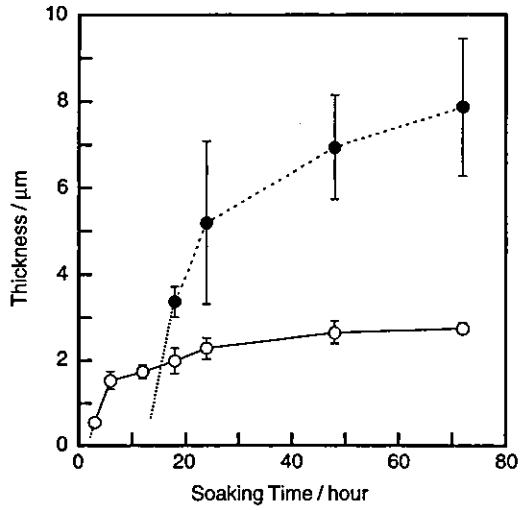

Fig. 4 Relationship between thickness of b-HA layer and soaking time in SBF. (○) sample A (the sponge) and (●) sample B.

b-HA particles on these substrates was measured using at least five points in SEM micrographs of their fracture faces and the mean thickness of b-HA particles and the standard deviation were shown. The induction period for b-HA formation on sample A is shorter than that of sample B. However, the crystal growth rate on sample B is higher than that on sample A.

When the sample A is soaked in SBF, the surface area of CCPC increases after the rapid dissolution of sucrose particles. This is suggested to be increased in the adsorption amount of Ca^{2+} and P^{5+} ions in SBF on the sponge skeleton. Figure 5 shows the amount of Ca^{2+} and P^{5+} ions after soaking sample A or sample B in SBF for various periods. When sample A is soaked, the Ca^{2+} ion amount in SBF increases slightly at the initial stage, and subsequently decreases gradually. It is proposed that the amount of the dissoluble vaterite particles, which come into contact with water, increases after dissolution of sucrose, resulting in the increase in the amount of Ca^{2+} ion released in SBF. On the other hand, after sample B is soaked in SBF, the Ca^{2+} ion amount decreases grádually. The P^{5+} ion amount in SBF

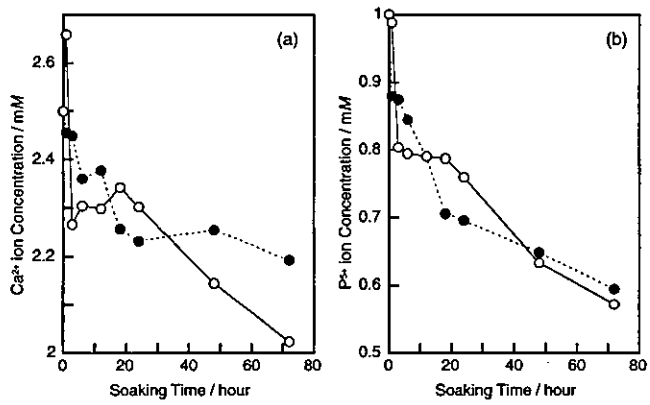

Fig. 5 Concentrations of (a) Ca^{2+} and (b) P^{5+} ions in 100 mL of SBF before and after soaking in SBF. (○) sample A (the sponge) and (●) sample B.

decreases gradually after soaking sample A or B. The phosphorous element in SBF is suggested to adsorb on CCPC as a phosphate ion.

The reduction of the induction period for b-HA formation on the CCPC sponge is suggested to be influenced by the porous structure. When the sample A is soaked in SBF, the surface area of CCPC increases due to the dissolution of the sucrose particles. As a result, a large amount of vaterite in the CCPC sponge skeleton rapidly dissolved. The pores in the sponge are considered as compartmental spaces with channels. In comparison with the surface of sample B, the supersaturation concerning b-HA around the surface of pores in the sponge (sample A) is suggested to increase rapidly. As a result, the induction period for b-HA formation on sample A is reduced. Figure 2(a) shows that the thickness of the sponge skeleton is in a range of 50~100 μm. Almost all of vaterite is dissolved within 1 hour after soaking (Fig. 1); almost no Ca^{2+} ions can be newly released from CCPC since 1 hour of soaking. As a result, the crystal growth rate on the sponge skeleton (sample A) may be suppressed. The b-HA growth rate may be also attributed to the surface area. The amount of carboxy group, which is known to induce b-HA nucleation,[13] increases with increase in surface area of the PLA portion due to the dissolution of sucrose and vaterite during the preparation of the sponge. The adsorption amount of the phosphate ion per unit surface area on the sponge skeleton may be smaller than that on the surface of sample B. As a result, the b-HA growth rate would be strictly suppressed.

Figure 6 shows a typical stress-strain curve measured by a compressive tester for the sponge prepared by soaking in SBF for 3 days. The sponge shows the compressive strength of ~1.5 MPa and the maximum strain for the fracture of the sponge is over 10%, which is two orders of magnitude larger than that of a dense hydroxyapatite ceramic.[14] The curve also shows that the fracture proceeds gradually beyond the maximum stress; the sponge leads to ductile fracture. The sponges in the present work are not broken in normal handling during operations.

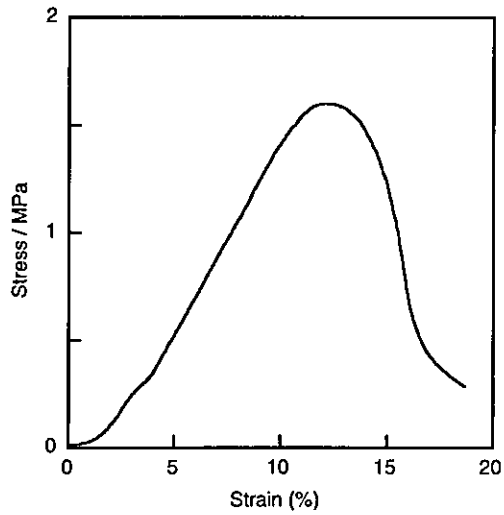

Fig. 6 Typical stress-strain curve in a compressive test of the sponge prepared by soaking in SBF for 3 days.

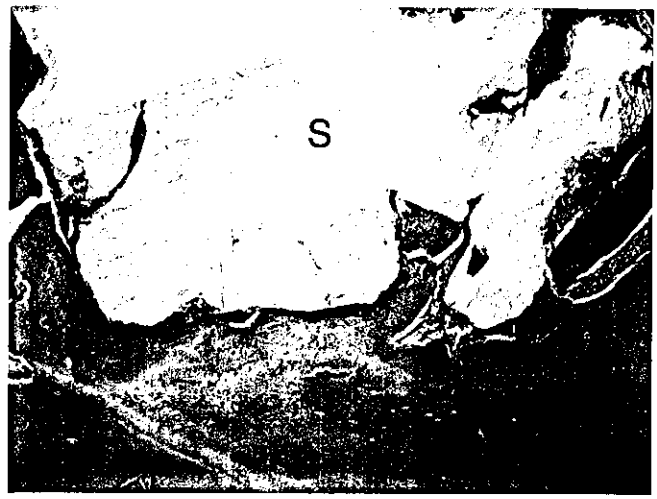

Fig. 7 The optical micrograph of a decalcified section of the sponge after implantation into a femur of a rat for 4 weeks. (S) the sponge, (NB) native bone, and (FB) newly formed bone. The section was stained with hematoxylin and eosin. Bar scale is 100 μm.

Figure 7 shows the decalcified sections stained with HE at 4 weeks postimplantation; newly bone formed in the pore. This figure shows that newly formed bone continues to be present in direct contact with the sponge without intervening soft tissues. No adverse tissue response and inflammation reaction were seen around the implant. The present osteoconducting sponge is also expected to have bioresorbability. Further histological investigation is in progress.

4. Conclusion

Coating with b-HA on CCPC sponge skeleton surface can be easily prepared in a short time utilizing a sucrose-particle-leaching technique combined with a biomimetic processing. The induction period for b-HA formation on the CCPC sponge skeleton is significantly shorter than that of a CCPC compact without sucrose. The sponge prepared using sucrose has numerous, large pores of 450~580 μm in diameter, which are connected with channels having a diameter in the range of 70~120 μm, as well as a high porosity of 75%. The sponge is expected to allow the migration of cells into the interior of the sponge. It is not broken in normal handling during operations. Animal test using rats showed that the present material has a osteoconductivity. The sponge is one of the great potential candidates as bone-fillers or scaffolds for tissue engineering.

Acknowledgements

The present work was supported in part by a Grant-in-Aid for Scientific Research from Japan Society for the Promotion of Science and by a grant from the NITECH 21st Century COE Program "World Ceramics Center for Environmental Harmony".

REFERENCES

1) T. Noshi, T. Yoshikawa, M. Ikeuchi, Y. Dohi, H. Ohgushi, K. Horiuchi, M. Sugimura, K. Ichijima and K. Yonemasu: J. Biomed. Mater. Res. 52

(2000) 621–630.
2) J. Dong, T. Uemura, Y. Shirasaki and T. Tateishi: Biomater. **23** (2002) 4493–4502.
3) T. Yoshikawa, H. Nakajima, E. Yamada, M. Akahane, Y. Dohi, H. Ohgushi, S. Tamai and K. Ichijima: J. Bone Miner. Res. **15** (2000) 1147–1157.
4) T. Kokubo: Acta Mater. **46** (1998) 2519–2527.
5) Y. Doi: Cells and Mater. **7** (1997) 111–122.
6) Y. Doi, T. Shibutani, Y. Moriwaki and Y. Iwayama: J. Biomed. Mater. Res. **39** (1998) 603–610.
7) H. R. Ramay and M. Zhang: Biomater. **24** (2003) 3293–3302.
8) R. Zhang and P. X. Ma: J. Biomed. Mater. Res. **45** (1999) 285–293.
9) J. A. Roether, A. R. Boccaccini, L. L. Hench, V. Maquet, S. Gautier and R. Jérôme: Biomater. **23** (2002) 3871–3878.
10) H. Maeda, T. Kasuga, M. Nogami, Y. Hibino, K. Hata, M. Ueda and Y. Ota: J. Mater. Res. **17** (2002) 727–730.
11) T. Kasuga, H. Maeda, K. Kato, M. Nogami, K. Hata and M. Ueda: Biomater. **24** (2003) 3247–3253.
12) K. Nakamae, S. Nishiyama, J. Yamashiro, Y. Fujimura, A. Urano and Y. Tosaki: Nihon-Setchaku-Kyokai-shi (in Japanese) **21** (1985) 414–450.
13) M. Tanahashi and T. Matsuda: J. Biomed. Mater. Res. **34** (1997) 305–315.
14) H. Aoki: *Mechanical Properties*, (Medical Application of Hydroxyapatite, Tokyo, 1994) pp. 286–306.

ELSEVIER

Science and Technology of Advanced Materials 6 (2005) 48-53

SCIENCE AND TECHNOLOGY OF ADVANCED MATERIALS

www.elsevier.com/locate/stam

Preparation of bonelike apatite composite for tissue engineering scaffold

Hirotaka Maeda[a], Toshihiro Kasuga[a,*], Masayuki Nogami[a], Minoru Ueda[b]

[a]*Department of Materials Science and Engineering, Graduate School of Engineering, Nagoya Institute of Technology, Gokiso-cho, Showa-ku, Nagoya 466-8555, Japan*

[b]*Nagoya University Graduate School of Medicine, Tsurumai-cho 65, Showa-ku, Nagoya 466-8550, Japan*

Received 8 March 2004; revised 7 June 2004; accepted 15 July 2004

Abstract

A novel sponge composed of a poly (lactic acid) composite skeleton covered with bonelike apatite (b-HA) was produced via a particle-leaching technique combined with a biomimetic processing. The sponge has a large porosity of ~75% with large-sized pores and shows mechanical ductility. After incubation of human osteoblasts for 7 days, numerous cells attached to the surface of the skeleton, which was covered with b-HA. One result of the osteoclastic cell culture showed that the b-HA on the composite has excellent bioresorbability. The sponge is expected to be one of the promising candidates for bone tissue engineering scaffolds.

Keywords: Bonelike apatite; Sponge; Poly(lactic acid); Vaterite; Simulated body fluid; Cell-compatibility

1. Introduction

While historically, organic tissue has been employed in the repair of bone defects; more recently, attention has been paid to synthetics, which may obviate the problems arising from the use of organic tissue in bone grafting. The use of all allografts carries the risk of disease transmission and tissue rejection, while autografts present problems of limited supply and donor site morbidity. These facts have made synthetic grafts an alternative to organic grafts. Some ceramics, such as Bioglass®, sintered hydroxyapatite and glass–ceramic A–W, have been shown to spontaneously bond to living bone [1–3]. They are called bioactive materials, and are already in clinical use as important bone-repairing materials. These materials could promote the generation of new bone by acting as a scaffold for osseous growth, but they are only osteoconductive and not osteoinductive.

Vacanti et al. have developed a new technique called 'tissue engineering' [4]. Engineering living tissue for reconstructive surgery requires an appropriate cell source, optimal culture conditions, and a biodegradable scaffold as the basic elements. A scaffolding material is used either to induce formation of bone from the surrounding tissue or to act as a carrier or template for implanted bone cells or other agents. To serve as a scaffold for bone tissue engineering, the material must be biocompatible, osteoconductive, and have a macroporous structure. Calcium phosphate ceramics such as hydroxyapatite or β-tricalcium phosphate (β-TCP), which have osteoconductivity, were reported to have been applied to scaffolds for bone tissue engineering [5,6].

Recently, much attention has been paid to bonelike hydroxycarbonate apatite (b-HA) as a novel biomaterial, since b-HA is very similar to apatite in terms of living bone in its chemical composition and structure [7] and shows effective compatibility in cell attachment, proliferation, and differentiation on the material [8], as well as good bioresorbability [9]. We expect that the sponges composed of b-HA skeleton can be applied to scaffolds for bone tissue engineering. In general, ceramics show brittleness and low resistance against impact loading. Such ceramic sponge materials have a serious risk of breaking in normal handling during operations. To eliminate this risk, it has been reported that the composites were fabricated using a polymer sponge coated with bioactive materials such as hydroxyapatite or Bioglass® [10,11].

* Corresponding author. Tel./fax: +81 52 735 5288.
E-mail address: kasuga.toshihiro@nitech.ac.jp (T. Kasuga).

1468-6996/$ - see front matter © 2005 Published by Elsevier Ltd.
doi:10.1016/j.stam.2004.07.003

A preparation method for b-HA using simulated body fluid (SBF), which is a tris-buffer solution with inorganic ion concentrations almost equal to those of human plasma, is called a biomimetic method [12]. This method has an advantage over conventional methods in that materials can be coated with b-HA without heating. Two indispensable conditions needed for the formation of b-HA on materials using SBF are (1) the existance of the surface functional groups that induce nucleation of b-HA and (2) increase in the supersaturation of b-HA in SBF [3,13,14].

Poly(lactic acid) (PLA) with many carboxy groups is one of the promising candidates for supplying inducers for the b-HA nucleation. A carboxy group, which is known to induce b-HA nucleation [13], can be formed by the hydrolyzation of PLA. To increase the supersaturation of b-HA in SBF, a large amount of Ca^{2+} ions should be dissolved from the materials. Bioresorbable calcium carbonate is expected to provide Ca^{2+} ions for SBF resulting in an increase in the supersaturation of b-HA. It is well known that calcium carbonate has three polymorphs, viz. calcite, aragonite and vaterite. The solubility of vaterite is higher than that of calcite or aragonite [15]. We have already reported that the PLA composites containing vaterite have much higher b-HA-forming ability in SBF than the composites containing calcite or aragonite without vaterite [16]. In our earlier work a pellet of a powder mixture consisting of 25 wt% biodegradable PLA and 75 wt% nano-sized calcium carbonate (vaterite) was reported to form b-HA on its surface even after being soaked for 3 h in SBF [17]. It was suggested that rapid formation of the b-HA originated from the fact that PLA contains carboxy groups that are bonded with Ca^{2+} ions for the b-HA nucleation, and a large amount of vaterite, which has the ability to effectively increase the supersaturation of the b-HA. We believe that various novel biomaterials can be prepared using PLA and vaterite. Hereafter, the composites are denoted by CCPC (Calcium Carbonate/Poly(lactic acid) Composites).

In the present work, we biomimetically prepared a novel sponge composed of PLA composite skeleton covered with b-HA utilizing CCPC. The present study also involves the evaluation of cell-compatibility on CCPC covered with b-HA for application to tissue engineering scaffolds.

2. Experimental method

2.1. Preparation of vaterite powders

Vaterite was prepared by a carbonation process using methanol [18]. CO_2 gas was blown for 3 h at a flow rate of 300 mL/min into the suspension consisting of 7.0 g of $Ca(OH)_2$ in 180 mL of methanol at 0 °C in a Pyrex® beaker. The resultant slurry was dried at 70 °C in air, resulting in fine-sized powders. Fig. 1 shows an X-ray diffraction (XRD) pattern and scanning electron microscopy (SEM) photograph of the vaterite powders. The XRD pattern shows that the calcium carbonate powders obtained in the present work consist predominantly of vaterite with small amounts of aragonite and calcite. The SEM photograph shows that secondary particles of $\leq$500 nm diameter were formed as an agglomeration of primary particles of ~100 nm. The BET surface area was measured to be ~40 m^2/g.

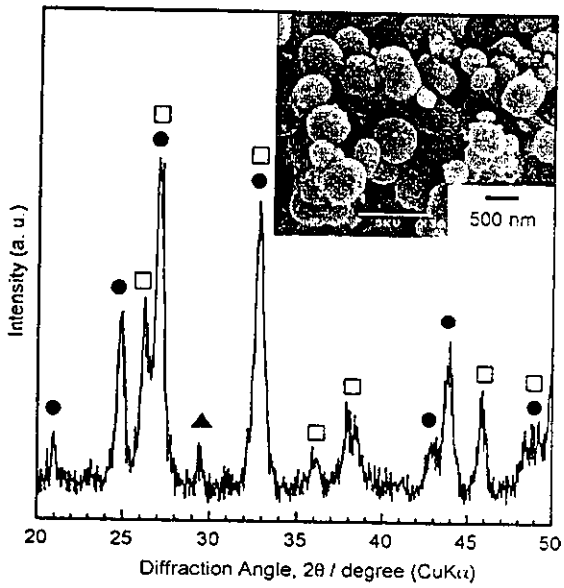

Fig. 1. The XRD pattern of vaterite powders prepared by a carbonation process in methanol. (●) vaterite, (▲) calcite, and (□) aragonite. Inset shows the SEM photograph of vaterite.

2.2. Preparation of PLA composites containing vaterite powders

PLA produced by Shimadzu Corp. (LACTY#2012) was used as a matrix phase. PLA with a molecular weight of 160±20 kDa, determined by gel permeation chromatography, was dissolved in methylene chloride at room temperature. The vaterite powders were added to the PLA solution and the mixture was then stirred. The weight ratio of vaterite/PLA was 1/2. We have already reported that CCPC containing ~30% vaterite has excellent mechanical properties, such as a bending strength of ~50 MPa, Young's modulus of ~5 GPa and ductility, with a high b-HA-forming ability in SBF [19]. The slurry mixture was stirred and cast into a stainless steel die, and then dried in air for solidification. After that, the product in the die was heated at 180 °C and uniaxially hot-pressed under a pressure of 40 MPa. After the heating, the specimen in the die was cooled to room temperature.

Fig. 2(a) shows a photo of CCPC in the present work. The sample was picked up and bent with two fingers. CCPC has high flexibility and can be cut using scissors, as shown in Fig. 2(b).

(a)

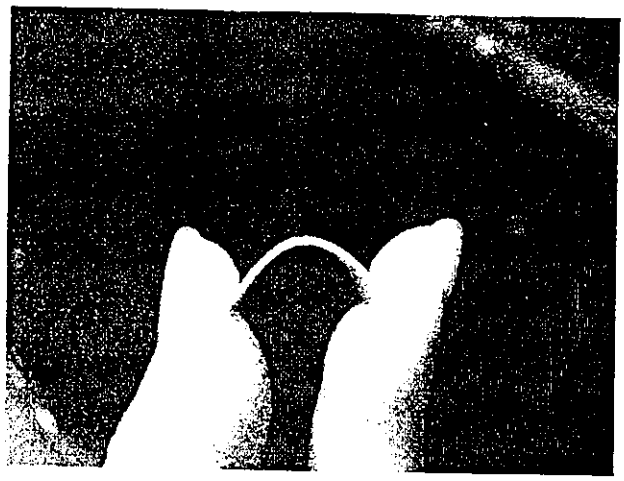

(b)

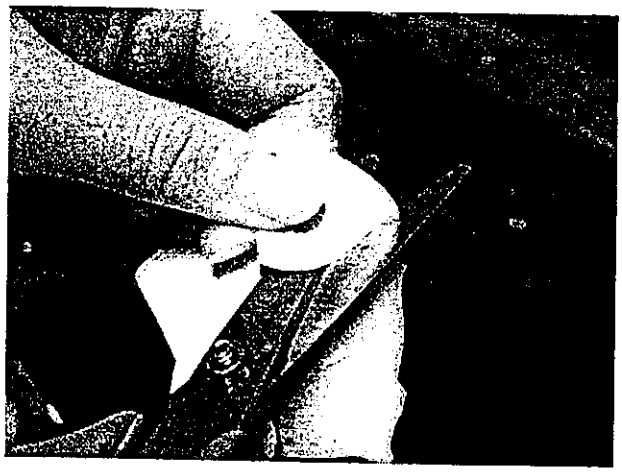

Fig. 2. Photos of (a) flexiblility test and (b) cutting test of CCPC.

2.3. Preparation of the CCPC sponge skeleton covered with b-HA

2.0 g of PLA was dissolved in 20 mL of methylene chloride at room temperature The vaterite powders were added to the PLA solution and the mixture was then stirred to prepare a PLA slurry including the vaterite powders. The weight ratio of vaterite/PLA was 1/2. The sponge was prepared using a conventional particle-leaching technique. In the present work sucrose was used as a sacrificial phase. Sucrose particles, which were sieved with an opening of from 0.5 to 1.0 mm, were added to the PLA slurry. The weight ratio of CCPC/sucrose was 1/6. The slurry mixture was stirred, cast into a stainless steel die, and subsequently dried in air for solidification. After that, the product in the die was heated at 180 °C and uniaxially hot-pressed at this temperature under a pressure of 40 MPa to prepare a CCPC/sucrose composite. After the hot-pressing, the specimen was cut in methanol with a diamond saw. Our strategy for the preparation of the sponge composed of CCPC skeleton coated with b-HA is to leach out the sucrose phase and to simultaneously form b-HA on the composite skeleton utilizing SBF (consisting of 2.5 mM of Ca^{2+}, 142.0 mM of Na^+, 1.5 mM of Mg^{2+}, 5.0 mM of K^+, 148.8 mM of Cl^-, 4.2 mM of HCO_3^-, 1.0 mM of HPO_4^{2-}, and 0.5 mM of SO_4^{2-}) that included 50 mM of $(CH_2OH)_3CNH_2$ and 45.0 mM of HCl at pH 7.4 at 37 °C as a solvent. The CCPC/sucrose composite was soaked in SBF for 3 days.

The crystalline phases in the sponge were identified by XRD, and the morphology of the sponge observed by SEM. The pore size distribution of the sponge was measured by mercury porosimetry. The compressive strength of the sponge (7×7×10 mm) was estimated by a compressing test at a loading rate of 1 mm/min.

2.4. Osteoblastic and osteoclastic cell cultures

Human bone marrow stromal cells, obtained by aspiration from the femoral diaphysis of patients were used for this experiment. The cell suspension was cultured in mesenchyaml stem cell basal medium (MSCBM, Camblex) with 10% fetal bovine serum (FBS) supplemented with 20 μg/mL L-glutamine, 1 μg/mL penicillin/streptomycine and incubated at 37 °C in a humidified atmosphere of 95% air and 5% CO_2. Two millilitres of a cell suspension containing (1×10^4 cell/mL) was plated on the CCPC sponge skeleton covered with b-HA (5×5×5 mm) and the sponge then incubated at 37 °C in 5% CO_2 for 1 week.

Osteoclasts were obtained from the long bones of 1-day-old neonatal rabbits (Japan white), following a reference [20]. A α-modified minimum essential medium (α-MEM, Gibco) supplemented with 15% FBS and antibiotics was used as the plating medium. A cell suspension (100 μL) containing 50–100 multinucleated osteoclasts/100 μL was plated onto disk shaped CCPC (with the composition of $CaCO_3$/PLA = 1/2 in weight ratio) covered with b-HA prepared by soaking in SBF for 2 days (8 mmØ × 1 mm) plated in the small wells of microculture plates. A compact of CCPC (with the composition of $CaCO_3$/PLA = 1/2 in weight ratio) was used as a control material to compare with CCPC covered with b-HA. After incubation at 37 °C in 5% CO_2 for 90 min, the unattached cells were gently washed off and the substrates were transferred into 35 mm culture medium and then incubated at 37 °C in 5% CO_2 for 2 days.

After the culturing period, the samples were fixed with glutaraldehyde in a cacodylate buffer. The cells, after being rinsed several times in the same buffer, were post-fixed in 1% osmium tetraoxide and dehydrated through graded ethanols. The samples were freeze-dried with *tert*-butyl alcohol and coated with osmium. The morphology of osteoblasts and osteoclasts, and the resorption lacunae produced by osteoclasts on the surface of the substrates were observed with SEM.

3. Results and discussion

3.1. CCPC sponge skeleton covered with b-HA

Fig. 3 shows the SEM photographs, the XRD pattern, and the pore size distribution of the sample following 3 days of soaking in SBF. The SEM photograph shows that the sponge has numerous, large pores of 450–580 μm in diameter and large interconnected channels of 70–120 μm. The sponge has continuous open foams with a 3D interpenetrating network of struts and pores, while the surface of the CCPC sponge skeleton is covered with numerous deposits. In Fig. 3(b), it is clear that, although an XRD peak of $2\theta \sim 32°$ resulting from the HA is not clear due to superimposition on the calcium carbonate (aragonite), the peak appears anew following the treatment (in comparison with the XRD pattern of the calcium carbonates in Fig. 1). That is, judged from the XRD pattern and the morphology, the deposits are concluded to be b-HA. The pore-size distribution measured using a mercury porosimeter showed that there exist almost no pores below several tens of micrometers in diameter and the median pore size of the sponge is 125 μm. The porosity was estimated from the measurement to be ~75%. When a compact of the powder-mixture consisting of CCPC and sucrose was hot-pressed at 180 °C, the sucrose particles melted (it begins to melt at 160 °C), leading to adjacent particles connecting to each other. As a result, both the sucrose and CCPC phases were unified into an interconnecting three-dimensional network. The macroporous structure of the sponge may allow the migration of cells into the interior of the sponge.

Fig. 4 shows typical stress–strain curves measured by a compressive tester for the CCPC sponge and β-TCP sponge with the same porosity of 75%. The CCPC sponge shows the compressive strength of ~1.5 MPa and the maximum strain for the fracture of the sponge is over 10%. The curve of the CCPC sponge also shows that the fracture proceeds gradually beyond the maximum stress; the sponge leads to ductile fracture. On the other hand, although the β-TCP sponge has strength close to that of the CCPC sponge, the stress–strain curve shows a typically brittle fracture. The CCPC sponge in the present work will not break in normal handling during operations. This ductility is believed to be an important mechanical property for the tissue engineering.

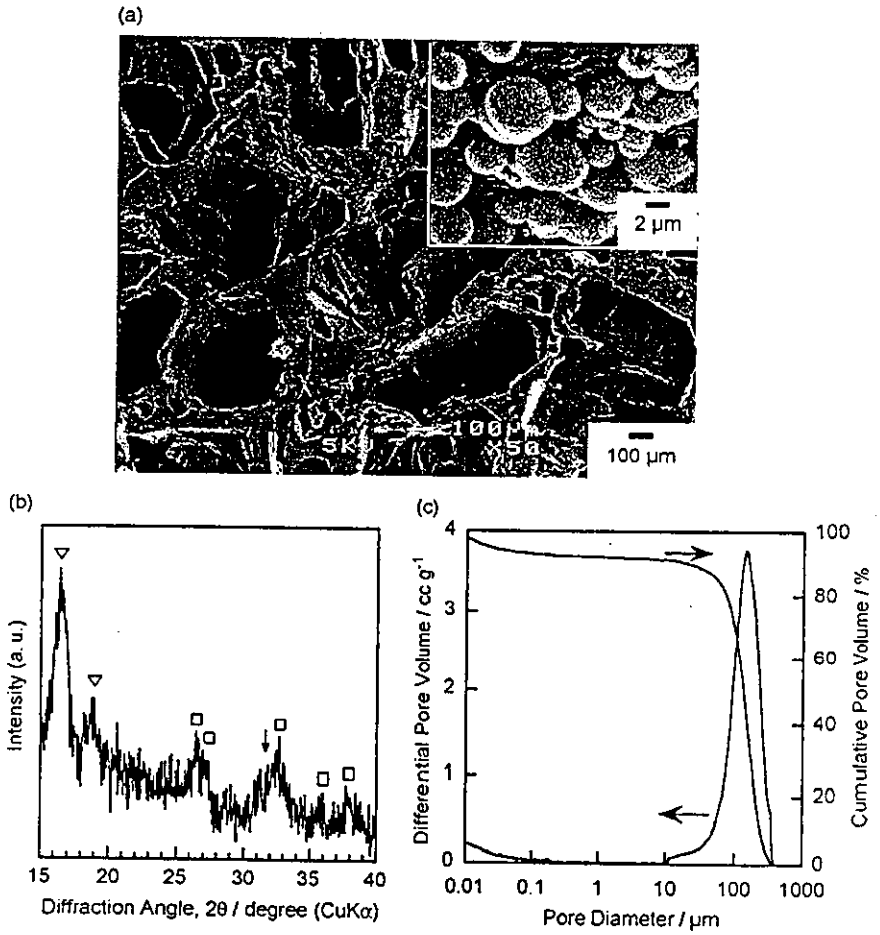

Fig. 3. (a) SEM photographs of the cut surface, (b) the XRD pattern, and (c) the pore size distribution of the sponge prepared in the present work.. (□) aragonite, (▽) PLA, and (↓) apatite. Inset shows the magnified image of the skeleton surface.

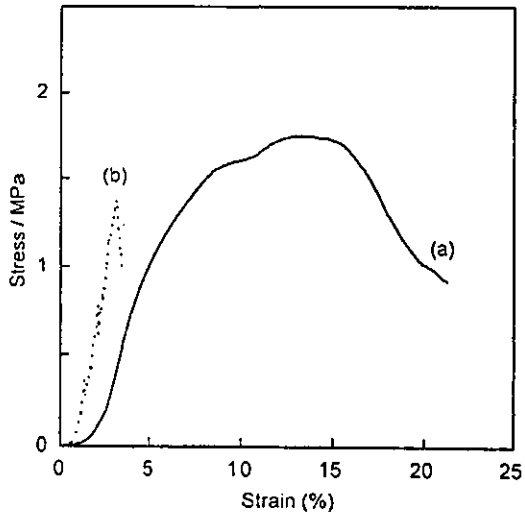

Fig. 4. Typical stress–strain curves of (a) the CCPC sponge and (b) β-TCP sponge in a compressive test.

3.2. Cells culture on CCPC

Fig. 5 shows a cross-sectional SEM photograph of the skeleton surface around the center of the CCPC sponge following one-week incubation. Numerous cells were attached to the skeleton covered with b-HA. We believe that cells can migrate through the channels into the interior of the sponge. SEM observation showed that the adhesion of cells on the skeleton covered with b-HA is larger than that on the sponge skeleton composed of PLA. This suggests that the presence of the b-HA layer on CCPC induces an effective increase in the attachment of the cells.

Fig. 6 shows SEM photographs of the osteoclast on the surface of CCPC covered with b-HA and CCPC after incubation for 2 days. The resorption lacuna was evident on the surface of these substrates. This area was widespread with a diameter of more than 25 μm on CCPC covered with b-HA. The attacks (~15 μm of diameter) on CCPC are

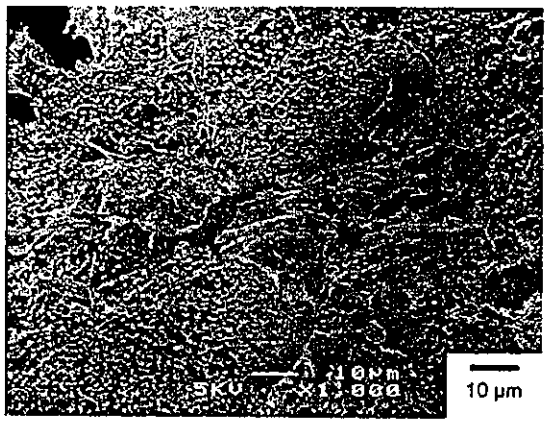

Fig. 5. The SEM photograph of the skeleton surface covered with b-HA around the center of the CCPC sponge after incubation of osteoblastic cells for one week.

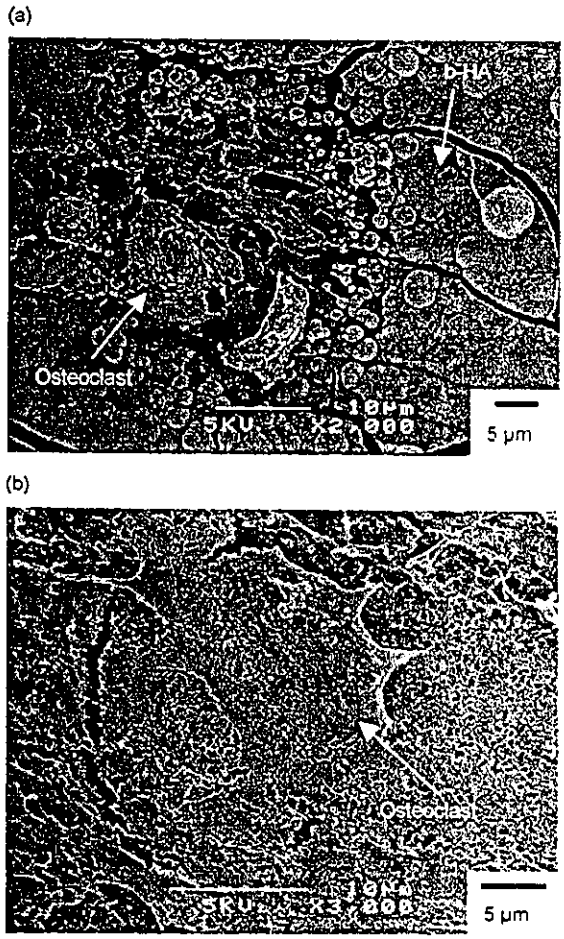

Fig. 6. The SEM photograph of the surface of (a) the CCPC covered with b-HA and (b) CCPC after incubation of osteoclastic cells for 2 days.

smaller than that on CCPC with b-HA. Although further statistical analysis concerning the difference between the lacuna sizes of the samples is needed, Fig. 6 clearly shows the different bioresorption behaviors; the b-HA layer on the CCPC increases the resorption produced by osteoclasts.

4. Conclusion

A novel sponge, covered with b-HA on its skeleton surface, was prepared using a particle-leaching technique combined with a biomimetic processing. The formed sponge has numerous, large pores of 450–580 μm in diameter, which are connected with channels having a diameter in the range of 70–120 μm, as well as a high porosity of 75%. The sponge is expected to allow the migration of cells into its interior, and is not broken in normal handling during operations. Cell-compatibility of the CCPC is greatly enhanced after induction of the formation of the b-HA layer. The sponge is one of the great potential candidates as scaffolds for bone tissue engineering.